

Hydrodynamics  
Section

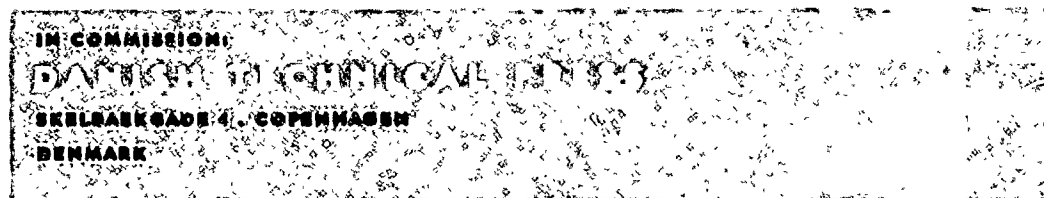


Report No. Hy-11 . November 1968

# Propeller Lifting-Surface Corrections

BY

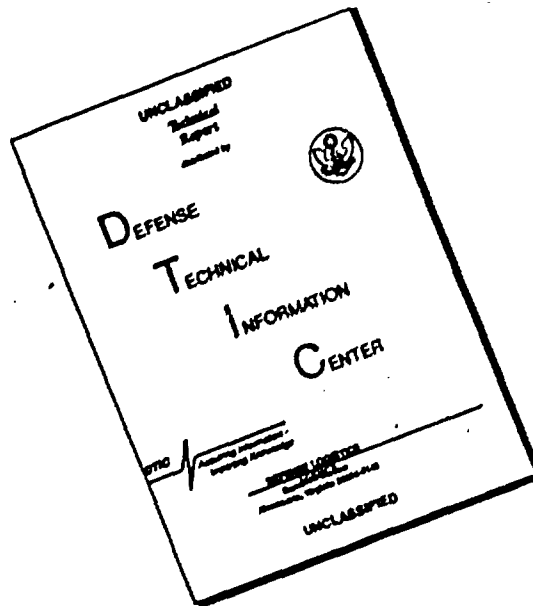
WM. B. MORGAN,  
VLADIMIR ŠILOVIĆ, and  
STEPHEN B. DENNY



Hy-11

Reproduced by the  
CLEARINGHOUSE  
for Federal Scientific & Technical  
Information Springfield Va 22151

# DISCLAIMER NOTICE



THIS DOCUMENT IS BEST QUALITY AVAILABLE. THE COPY FURNISHED TO DTIC CONTAINED A SIGNIFICANT NUMBER OF PAGES WHICH DO NOT REPRODUCE LEGIBLY.

## HYDRO- OG AERODYNAMISK LABORATORIUM

is a self-supporting institution, established to carry out experiments for industry and to conduct research in the fields of Hydro- and Aerodynamics. According to its by-laws, confirmed by His Majesty the King of Denmark, it is governed by a council of eleven members, six of which are elected by the Danish Government and by research organizations, and five by the shipbuilding industry.

Research reports are published in English in two series: **Series Hy** (blue) from the Hydrodynamics Section and **Series A** (green) from the Aerodynamics Section.

The reports are on sale through the Danish Technical Press at the prices stated below. Research institutions within the fields of Hydro- and Aerodynamics and public technical libraries may, however, as a rule obtain the reports free of charge on application to the Laboratory.

The views expressed in the reports are those of the individual authors

### Series Hy:

No.:	Author:	Title:	Price: D. Kr.
Hy-1	PROHASKA, C. W.	Analysis of Ship Model Experiments and Prediction of Ship Performance (Second printing)	5,00
Hy-2	PROHASKA, C. W.	Trial Trip Analysis for Six Sister Ships	6,00
Hy-3	ŠILOVIĆ, V.	A Five Hole Spherical Pitot Tube for Three Dimensional Wake Measurements	6,00
Hy-4	STRØM-TEJSEN, J.	The HyA ALGOL-Programme for Analysis of Open Water Propeller Test	6,00
Hy-5	ABKOWITZ, M. A.	Lectures on Ship Hydrodynamics — Steering and Manoeuvrability	20,00
Hy-6	CHISLETT, M. S., and STRØM-TEJSEN, J.	Planar Motion Mechanism Tests and Full-Scale Steering and Manoeuvring Predictions for a MARINER Class Vessel	12,00
Hy-7	STRØM-TEJSEN, J., and CHISLETT, M. S.	A Model Testing Technique and Method of Analysis for the Prediction of Steering and Manoeuvring Qualities of Surface Vessels	12,00
Hy-8	CHISLETT, M. S., and BJØRHEDEN, O.	Influence of Ship Speed on the Effectiveness of a Lateral-Thrust Unit	12,00
Hy-9	BARDARSON, H. R., WAGNER SMITT, L., and CHISLETT, M. S.	The Effect of Rudder Configuration on Turning Ability of Trawler Forms: Model and Full-Scale tests with special reference to a Conversion to Purse-Seiners	20,00
Hy-10	WAGNER SMITT, L.	The Reversed Spiral Test. A Note on Bech's Spiral Test and some Unexpected Results of its Applications to Coasters	10,00
Hy-11	WM. B. MORGAN, VLADIMIR ŠILOVIĆ, and STEPHEN B. DENNY	Propeller Lifting-Surface Corrections	25,00

# Propeller Lifting-Surface Corrections

by

WM. B. MORGAN,  
VLADIMIR ŠILOVIĆ, and  
STEPHEN B. DENNY



HYDRO- OG AERODYNAMISK LABORATORIUM  
LYNGBY  
DENMARK

## TABLE OF CONTENTS

	Page
Introduction .....	1
Theoretical Background .....	3
Presentation of the Series .....	8
Experimental Checks on the Theory .....	20
Conclusions .....	27
Acknowledgments .....	28
References .....	28

## PREFACE

During the summer of 1967 Dr. Wm. B. Morgan, Naval Architect, Hydro-mechanic Laboratory, Naval Ship Research and Development Center, Washington, D. C., spent three months at the Hydro- and Aerodynamics Laboratory. Although his stay was short it became very fruitful. Besides giving lectures on Propeller Design at the Technical University of Denmark he found time to prepare in co-operation with Dr. V. Šilović, Head of Propeller Section at HyA, the present paper on Propeller Lifting-Surface Corrections, which was finalised after Dr. Morgan's return to the N.S.R.D.C. with the further assistance of Mr. Stephen B. Denny, mathematician, N.S.R.D.C.

The Hydro- and Aerodynamics Laboratory is grateful to the Naval Ship Research and Development Center for having made this co-operation possible, also to the Applied Mathematics Laboratory of N.S.R.D.C., and to the Northern Europe University Computing Centre, Lyngby, Denmark, for assistance in the numerical calculations.

PROHASKA

Professor, Dr. techn.  
Director, Hydro- and  
Aerodynamisk Laboratory

AD 687670

## Propeller Lifting-Surface Corrections

By Wm. B. Morgan,<sup>1</sup> Member, Vladimir Silovic,<sup>2</sup> Member, and Stephen B. Denny,<sup>3</sup> Visitor

Correction factors for camber, ideal angle due to loading, and ideal angle due to thickness, which are based on propeller lifting surface theory, are presented for a series of propellers. This series consists of optimum free-running propellers with chordwise loadings the same as an NACA  $\alpha = 0.8$  mean line and with NACA-66 chordwise thickness distributions. The results of the calculations show that the three-dimensional camber and ideal angle are generally greater than the two-dimensional camber and ideal angle at the same lift coefficient. The correction factors increase with increasing expanded area ratio, and those for camber and ideal angle due to loading decrease with increasing number of blades. Thickness, in general, induces a positive angle to the flow, which necessitates a correction to the blade pitch. This ideal angle is largest near the blade root and decreases to negligible values toward the blade tip and increases with increasing number of blades. Skew induces an inflow angle, necessitating a pitch change which is positive toward the blade root and negative toward the blade tip.

### Introduction

THE trend in ships has been toward increasing speed, size, and horsepower. As a result, there is an increasing demand for the design of propellers which are efficient and yet produce minimum cavitation and induced vibration. Such a task requires a knowledge of the flow field in which a propeller operates and an accurate determination of the flow over the propeller blade surfaces.

Much effort has been devoted recently to the development of a more sophisticated propeller theory. This theory has proceeded from the simple momentum concepts of Rankine [1]<sup>4</sup> (1865) to the lifting-line model of Goldstein [2] (1929) and, finally, to the lifting-surface model of

Ludwig and Ginzel [3] (1944). More recently, because of the numerical evaluations possible with high-speed computers, emphasis has been placed on more sophisticated mathematical models than hitherto possible; e.g., Sparenberg [4], Cox [5], Pien [6], and Kerwin [7].

A complete review of the various lifting-surface theories will not be given here since adequate reviews for work through 1964 are given by Wu [8], Isay [9], and Lerbs et al. [10]. Recent work not mentioned in these three references are studies by Cheng [11, 12], Kerwin and Leopold [13], Nelson [14, 15], Sulmont [16, 17], Nishiyama and Sasajima [18], Malavard and Sulmont [19], and Murray [20]. Murray develops the lifting-surface theory of both contrarotating and conventional propellers.

In general, the investigators have dealt with the same basic mathematical model but have used different assumptions to obtain numerical solutions. The propeller-blade boundary conditions are linearized and the blade and its helical wake are replaced by vortex systems. Assumptions are made for the chordwise and spanwise loading on the blade and a complicated singular integral is derived from which the necessary distortion

<sup>1</sup> Naval Architect, Hydromechanics Laboratory, Naval Ship Research and Development Center, Washington, D. C.

<sup>2</sup> Naval Architect, Hydro-og Aerodynamisk Laboratorium, Lyngby, Denmark.

<sup>3</sup> Mathematician, Hydromechanics Laboratory, Naval Ship Research and Development Center, Washington, D. C.

<sup>4</sup> Numbers in brackets designate References at end of paper.

For presentation at the Annual Meeting, New York, N. Y., November 13-16, 1968, of THE SOCIETY OF NAVAL ARCHITECTS AND MARINE ENGINEERS.

to the blade can be calculated to obtain the prescribed loading. In addition to determining loading effects, Kerwin and Leopold [21], Nelson [14], and Murray [20] also considered the effect of blade thickness, in the linearized sense, and found that it contributed significantly to the required blade distortion.

For an unskewed propeller blade, the effect of loading on the blade shape is to require both a larger camber and a larger ideal angle than would be required in two-dimensional flow in order to produce the same lift. The principal effect of thickness is to distort the flow such that an increase in angle of the blade is required to maintain the desired loading. Likewise, the principal effect of skew is to necessitate a blade angle change but to require little change in camber.

Because of the linearized boundary conditions, camber and ideal angle corrections, which are independent of the magnitude of the propeller loading [10], can be derived by taking a ratio of the three-dimensional camber and ideal angle to the two-dimensional camber and ideal angle, respectively. These correction factors are, of course, dependent upon the chordwise and spanwise load (or pitch) distributions, number of blades, and blade area and shape. Similarly, a thickness correction factor can be derived which is independent of the magnitude of the thickness but is, of course, dependent upon the chordwise and spanwise thickness distributions.

Since lifting-surface correction factors can be derived which are independent of the magnitude of the propeller loading and thickness, a system-

## Nomenclature

- |  |   |
|--|---|
| <p> <math>A_E</math> = blade expanded area<br/> <math>A_0</math> = propeller disk area<br/> <math>BTF</math> = blade-thickness fraction<br/> <math>C(r)</math> = coefficient of blade outline<br/> <math>C_L</math> = lift coefficient, <math>\frac{2\pi G(r)VD}{cV_r}</math><br/> <math>C_{max}</math> = two-dimensional maximum mean-line ordinate for <math>C_L = 1.0</math><br/> <math>C_P</math> = power coefficient, <math>\frac{P_D}{\frac{\rho}{2}A_0V_A^3}</math><br/> <math>C_{Th}</math> = thrust coefficient, <math>\frac{T}{\frac{\rho}{2}A_0V_A^3}</math><br/> <math>c</math> = section chord<br/> <math>D</math> = propeller diameter<br/> <math>f</math> = two-dimensional camber ordinate<br/> <math>f_{max}</math> = maximum two-dimensional camber ordinate<br/> <math>f_p(r, x_c)</math> = maximum camber ordinate<br/> <math>f_p(r, x_c)</math> = chordwise camber ordinate<br/> <math>f_{D1}(r, x_c)</math> = camber ordinate induced by thickness<br/> <math>\tilde{f}(r, x_c)</math> = chordwise camber normalized by maximum camber<br/> <math>G(r)</math> = dimensionless circulation from lifting-line theory, <math>\Gamma(r)/\pi DV</math><br/> <math>G_r(r, \theta)</math> = dimensionless circulation over lifting surface, <math>\Gamma(r, \theta)/\pi DV</math><br/> <math>G_f(r)</math> = dimensionless circulation of helical free vortices<br/> <math>G_f(r, \theta)</math> = dimensionless circulation of helical free vortices over lifting surfaces<br/> <math>k_c(r)</math> = camber correction<br/> <math>k_i(r)</math> = angle-of-attack correction for thickness<br/> <math>k_a(r)</math> = ideal angle-of-attack correction<br/> <math>n</math> = revolutions per unit time<br/> <math>P_D</math> = propeller power<br/> <math>P_i</math> = hydrodynamic pitch<br/> <math>R</math> = propeller radius </p> | <p> <math>r</math> = radial coordinate nondimensionalized by propeller radius<br/> <math>r_h</math> = dimensionless hub radius<br/> <math>(r, \theta, z)</math> = dimensionless cylindrical coordinates<br/> <math>T</math> = propeller thrust<br/> <math>t(r, x_c)</math> = half-thickness ordinate<br/> <math>t_{max}(r)</math> = maximum-thickness ordinate<br/> <math>U(r)</math> = resultant induced velocity from lifting-line theory<br/> <math>U_n(r)</math> = velocity induced by loading normal to blade-section chord<br/> <math>U_{n1}(r)</math> = velocity induced by thickness normal to blade-section chord<br/> <math>U_T(r)</math> = tangential induced velocity<br/> <math>V</math> = ship speed<br/> <math>V_A(r)</math> = speed of advance at a given radius<br/> <math>V_i(P)</math> = induced velocity vector<br/> <math>V_r(r)</math> = resultant section inflow velocity<br/> <math>w(r)</math> = circumferential mean-wake coefficient at a given radius<br/> <math>(x, y, z)</math> = dimensionless cartesian coordinates<br/> <math>x_c</math> = chordwise section abscissa nondimensionalized by chord<br/> <math>x_{max}</math> = chordwise position of maximum camber<br/> <math>Z</math> = number of blades<br/> <math>\alpha_i(r)</math> = section ideal angle of attack<br/> <math>\alpha_{i,0}</math> = two-dimensional ideal angle of attack for <math>C_L = 1.0</math><br/> <math>\alpha_t(r)</math> = angle-of-attack correction from thickness<br/> <math>\beta_i(r)</math> = hydrodynamic pitch angle<br/> <math>\lambda_i</math> = induced advance coefficient = <math>r \tan \beta_i</math><br/> <math>\lambda_a</math> = apparent advance coefficient, <math>\frac{V}{\pi n D}</math><br/> <math>\sigma(r, )</math> = source strength<br/> <math>\theta_l(r)</math> = angular position of blade-section leading edge<br/> <math>\theta_s</math> = skew at blade tip, deg<br/> <math>\theta_t(r)</math> = angular position of blade-section trailing edge </p> |
|--|---|



atic series of these correction factors can be calculated for design use. By varying such parameters as blade number, blade area, blade skew, and hydrodynamic pitch angle, the effect of these parameters for a practical blade shape can be ascertained and a better understanding of the flow over the blade will result. These correction factors can be utilized in propeller design to obtain the blade pitch and camber without empirical adjustments. Design methods—developed over the years—based on empirical correction factors and on correction factors from simplified mathematical models should be regarded as outmoded.<sup>5</sup> In addition to providing the designer with coefficients with which he can design propellers by modern theoretical methods, these correction factors can be used for making qualitative checks of lifting-surface computer calculations, provided that the propeller geometry and loading do not differ radically from the series.

Lifting-surface correction factors are presented for four, five, and six blades, for blade area ratios from 0.35 to 1.15, for hydrodynamic pitch ratios from 0.4 to 2.0, and for three blade skews. The calculations are for optimum<sup>6</sup> free-running propellers and the results are similar to those presented by Lerbs [10] but with two essential differences. One is that the assumed chordwise load distribution is that of the NACA  $a = 0.8$  mean line: i.e., constant loading from the leading edge to 0.8 chord and then a constant slope to zero at the trailing edge. The second difference is the inclusion of a correction for thickness. Experimental results have shown that these differences are significant in applying lifting-surface theory to practical propeller designs. The thickness correction must be included if the propeller is to have sufficient pitch, and the NACA  $a = 0.8$  mean line is a mean line which achieves, approximately, its theoretical lift in viscous flow. For example, the NACA  $a = 1.0$  mean line achieves only 74 percent of its theoretical lift in a real fluid, and it is not feasible in the present lifting-surface theory to account for viscous effects on lift. In analogy with two-dimensional results, the NACA  $a = 0.8$  load distribution requires an ideal angle for the mean line to operate at shock-free entry.

<sup>5</sup> Reference [22] is an example of an outmoded method. In this particular reference the camber correction factors  $k_1$  and  $k_2$  are replaced by the camber correction factor  $k_c$ , and the pitch correction procedure is replaced by the ideal angle due to loading and thickness.

<sup>6</sup> The word optimum used here means the propeller has a constant hydrodynamic pitch. Strictly speaking, such a propeller would be optimum only when lightly loaded, when operating in an inviscid fluid, and if it had an infinite number of blades.

The following sections of the paper will review briefly the theory used for the calculations and outline the assumptions and limitations. Results of the calculations will be discussed. Some comparisons between experiment and theory will be presented and conclusions will be drawn from the apparent trends as to the applicability of the theory.

## Theoretical Background

### Statement of the Problem

The problem can be stated as follows: "For a given number, loading, area, skew, chord distribution, and thickness distribution, determine the required blade-section camber and ideal angle." This problem is similar to the inverse problem of airfoil theory, except that the thickness is specified.

### Assumptions

The brief theoretical background presented here will serve only to bring out the salient features of the procedures used. Details of the theories involved are available in references [12] and [21].

In the mathematical model for loading, a distribution of bound vortices is assumed to cover the blades, and free vortices are shed from these bound vortices downstream along helical paths. For thickness, a network of sources and sinks is assumed to be distributed over the blades. The following assumptions based on this mathematical model are generally made:

- 1 The fluid is inviscid and incompressible.
- 2 The free-stream velocity is axisymmetric and steady, allowing the propeller to be wake-adapted.
- 3 Each propeller blade is replaced by a distribution of bound vortices for loading effects, and sources and sinks for thickness effects. The circulation is distributed in both the chordwise and spanwise directions. It follows from vortex theory that free vortices are shed from the bound vortices and, in a coordinate system which rotates with the propeller, these free vortices form a general helical surface behind the propeller.
- 4 Each of the free vortices has a constant diameter and a constant pitch in the downstream direction, but the pitch may vary in the radial direction. This means that effects of slipstream contraction and centrifugal force on the shape of the free-vortex sheets are ignored.
- 5 The boundary conditions on the blade are linearized, which implies that the lifting surface

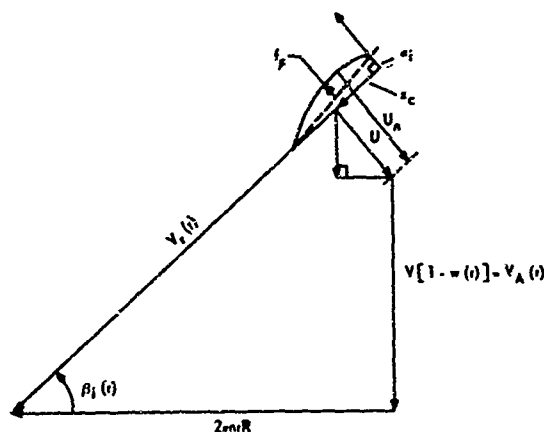


Fig. 1 Propeller velocity diagram

has only a small deviation from the hydrodynamic pitch. This assumption is similar to the linearized theory of two-dimensional airfoils where the boundary condition is not satisfied on the profile but on the profile chord. Also, the linearization enables separation of the loading and thickness effects.

6 The pitch of the blade and of the trailing vortex sheets is the hydrodynamic pitch obtained from lifting-line theory. Within the context of the linearized boundary conditions, this is not an assumption—except for skewed propellers—since the lifting-line theory does not account for skew.

7 The hub is assumed to be small enough that it is not necessary to satisfy the hub boundary condition.

8 Blade rake is not considered.

The assumptions listed apply to moderately loaded propeller theory. Assumption 4 would have to be removed for heavily loaded propellers, and an additional assumption would have to be made for lightly loaded propellers; namely, that the effect of the induced velocities on the pitch of the vortex sheets is negligible.

#### Loading

Fig. 1 shows the velocity diagram for a propeller blade section in the absence of thickness. From this figure and within the concepts of linearized theory, the boundary condition at each section is

$$\alpha_i(r) + \frac{\partial f_p(r, x_c)}{\partial x_c} = \frac{U_n}{V_r}(r, x_c) - \frac{U}{V_r}(r) \quad (1)$$

where  $f_p$  is the camber along the chord  $x_c$ ,  $\alpha_i$  is the ideal angle of attack ( $\alpha_i \approx \tan \alpha_i$ ),  $V_r$  is the re-

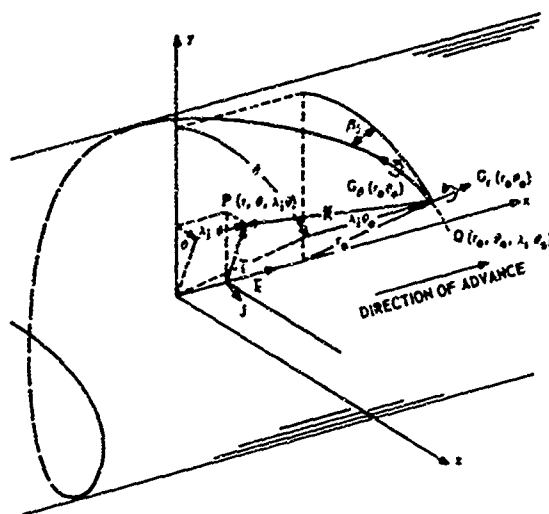


Fig. 2 Coordinate system

sultant inflow velocity to the blade section,  $U$  is the resultant induced velocity from lifting-line theory, and  $U_n$  is the induced velocity normal to the blade-section chord. The angle  $\beta_i$  shown in Fig. 1 is the hydrodynamic pitch angle.

Both a cartesian coordinate system ( $x, y, z$ ) and a cylindrical system ( $r, \theta, z$ ) will be used (see Fig. 2). The bound circulation will be assumed to have the strength  $G_r(r)$  such that

$$\int_{\theta_i(r)}^{\theta_t(r)} G_r(r, \theta) d\theta = G(r) \quad (2)$$

The coordinates  $\theta_i(r)$  and  $\theta_t(r)$  define the angular position of the blade-section leading and trailing edges, respectively, and  $G(r)$  is the non-dimensionalized bound circulation as determined from lifting-line theory [23]. Since  $G_r(r, \theta)$  may vary in both the radial and chordwise directions, a free vortex may be shed at each point on the blade surface and will trail behind along a helix of pitch  $\pi r \tan \beta_i$  ( $\tan \beta_i$  from lifting-line theory).

It follows from vortex theory that the strengths of the helical free vortices are equal to the negative of the radial rate of change of the bound circulation at the point the vortex is shed. If the strength of each helical free vortex is assumed to be  $G_f(r)$  behind the trailing edge, then

$$G_f(r) = - \frac{dG(r)}{dr} \quad (3)$$

With this equation and equation (2), the strengths of the free vortices shed from the blade are found to be

$$\begin{aligned}
G_f(r) &= -\frac{d}{dr} \int_{\theta_1(r)}^{\theta_2(r)} G_r(r, \theta) d\theta dr \\
&= -\int_{\theta_1(r)}^{\theta_2(r)} \frac{\partial G_r(r, \theta)}{\partial r} d\theta dr - G_r(r, \theta_1) \\
&\quad \times \frac{d\theta_1}{dr} dr + G_r(r, \theta_2) \frac{d\theta_2}{dr} dr \quad (4)
\end{aligned}$$

The first term on the right corresponds to the integral of the free vortex strengths from the leading edge to the trailing edge, which results from a radial change in the bound vortices. The two remaining terms on the right are strengths of the free vortices shed along the blade outline. It follows from this equation that, within the lifting surface, the free vortices have strength

$$\begin{aligned}
G_f(r, \theta) &= -G_r(r, \theta) \frac{d\theta_1}{dr} \\
&\quad - \int_{\theta_1}^{\theta_2(r)} \frac{\partial G_r}{\partial r}(r, \theta_0) d\theta_0 dr, \quad \theta_1 \geq \theta > \theta_2 \quad (5)
\end{aligned}$$

From the Biot-Savart law, the induced velocity  $V_i$  at any point  $P$  on the lifting surface is found to be

$$\begin{aligned}
\frac{V_i(P)}{V} &= -\frac{1}{2} \iint_{A_1}^{\text{bound vortices}} G_r(r, \theta) \left( \frac{\mathbf{S} \times d\mathbf{r}}{S^3} \right) d\theta \\
&\quad - \frac{1}{2} \iint_{A_1+A_2}^{\text{free vortices}} G_f(r, \theta) \left( \frac{\mathbf{S} \times d\mathbf{l}}{S^3} \right) dr \quad (6)
\end{aligned}$$

where  $A_1$  is the area of the lifting surface,  $A_2$  is the area of the helical surface behind the trailing edge of the blade,  $V$  is the freestream velocity or ship speed,  $\mathbf{S}$  is the vector distance from a point  $Q$  on the helical surface to the point  $P$  also on the helical surface,  $d\mathbf{l}$  is the elementary vector tangent to the vortex line, and  $S = |\mathbf{S}|$ . The second term in this equation can be expressed in two parts by equations (3) and (5), and the quantity

$$\frac{1}{2} \iint_{A_2} \frac{dG(r)}{dr} \left( \frac{\mathbf{S} \times d\mathbf{l}}{S} \right) dr$$

is now added to and subtracted from this equation;  $A_2$  is the area between the trailing edge and a generating line along which a lifting line would be placed. A new coordinate system is introduced such that the point  $P$  always lies on the lifting surface<sup>7</sup> [6]. This means that the integral

<sup>7</sup> For this change in coordinate system, the lifting line may deviate from the blade surface at radial points other than  $P$  when the propeller is not of constant pitch. The effect on the results is probably small if the pitch does not deviate too much from a constant value.

$$\frac{1}{2} \iint_{A_2+A_1} \frac{dG(r)}{dr} \left( \frac{\mathbf{S} \times d\mathbf{l}}{S^3} \right) dr \equiv \left( \frac{V_i}{V} \right)_{\text{lifting line}}$$

is identical to the velocity induced at a lifting line by the trailing vortex system. The velocity induced by the lifting surface itself is

$$\begin{aligned}
\frac{V_i(P)}{V} &= -\frac{1}{2} \iint_{A_1} G_r(r, \theta) \left( \frac{\mathbf{S} \times d\mathbf{r}}{S^3} \right) d\theta \\
&\quad + \frac{V_i}{V_{\text{lifting line}}} + \iint_{A_1} \left\{ G_r(r, \theta) \frac{d\theta_1}{dr} \right. \\
&\quad \left. + \int_{\theta_1}^{\theta_2(r)} \frac{\partial G_r}{\partial r}(r, \theta_0) d\theta_0 \right\} \left( \frac{\mathbf{S} \times d\mathbf{l}}{S} \right) dr \\
&\quad - \iint_{A_2} \frac{dG(r)}{dr} \left( \frac{\mathbf{S} \times d\mathbf{l}}{S^3} \right) dr \quad (7)
\end{aligned}$$

This equation gives the velocity induced by a single blade at the point  $P$ . The total velocity induced by all the blades at the point  $P$  on one of the blades is obtained by summing this equation with respect to the blade position  $m$ , of which  $\mathbf{S}$  is a function. The velocity  $V_i(P)$  includes the radial induced velocity as well as the axial and tangential velocities. The radial velocity does not appear in the boundary condition, equation (1), and can be neglected. Then, the normal velocity is

$$\mathbf{n} \cdot \frac{\mathbf{V}_i}{V_{\text{lifting line}}} \equiv \frac{V_r}{V} - \frac{U}{V_r}$$

and the equation which must be evaluated in determining  $\partial f_p / \partial x_c$  is

$$\begin{aligned}
\frac{V_r}{V} \left( \alpha_i + \frac{\partial f_p}{\partial x_c} \right) &= \frac{U_n(r, x_c)}{V} - \frac{U(r)}{V_r} = \\
&\quad - \frac{1}{2} \mathbf{n} \cdot \left\{ \sum_{m=1}^Z \iint_{A_1} G_r(r, \theta) \left( \frac{\mathbf{S} \times d\mathbf{r}}{S^3} \right) d\theta \right. \\
&\quad \left. + \frac{1}{2} \sum_{m=1}^Z \left[ \iint_{A_1} \left\{ G_r(r, \theta) \frac{d\theta_1}{dr} + \int_{\theta_1}^{\theta_2(r)} \frac{\partial G_r}{\partial r}(r, \theta_0) d\theta_0 \right\} \left( \frac{\mathbf{S} \times d\mathbf{l}}{S} \right) dr \right. \right. \\
&\quad \left. \left. - \iint_{A_2} \frac{dG(r)}{dr} \left( \frac{\mathbf{S} \times d\mathbf{l}}{S^3} \right) dr \right] \right\} \quad (8)
\end{aligned}$$

where  $Z$  is the number of blades. The blade camber is given by

$$f_p(r, x_c) + x_c \alpha_i(r) = \int_0^{x_c} \left[ \frac{U_n(r, \theta)}{V_r} - \frac{U(r)}{V_r} \right] d\theta \quad (9)$$

To determine  $\alpha_i$ , this integral is evaluated from the leading edge to the trailing edge and  $f_p$  is taken to be zero.

The equation for the slope of the camber line, equation (9), avoids integration limits of infinity, but the double integrals are difficult to evaluate because the integrands are singular when  $S$  becomes zero. To facilitate the numerical evaluation of these singular integrals, Pien [6] and Cheng [12] made a number of simplifications:

1 The radial bound circulation distribution  $G(r)$  and the hydrodynamic pitch ratio distribution are expanded in a half-range cosine series with a finite number of terms.

2 The singular points of the integrands are isolated and the integrals are evaluated numerically. In the region of the singular point, the radial integration is done analytically by assuming that pitch and circulation are constant.

3 For calculating the blade mean line, the induced normal velocity is expressed as a power series.

The simplifications are numerical approximations and not assumptions made in the theory. The precise accuracy of the evaluations is difficult to ascertain.

Correction factors for camber and ideal angle due to loading which are independent of the magnitude of propeller loading can be derived by normalizing the three-dimensional camber and ideal angle by the two-dimensional section values. With regard to camber, only the correction factors for the maximum chordwise camber will be formed in this way. From equation (9), then

$$k_c(r) = \frac{f_p(r, x_{\max})}{f_{\max}} = \frac{1}{C_{\max} C_L} \times \left\{ \int_0^{x_{\max}} \left[ \frac{U_n(r, x)}{V_r} - \frac{U(r)}{V_r} \right] dx - x_{\max} \alpha_i(r) \right\} \quad (10)$$

where  $x_{\max}$  is the chordwise position of maximum camber,  $C_L$  is the blade-section lift coefficient, and  $f_{\max}$  is the two-dimensional maximum camber and equal to

$$f_{\max} = C_{\max} C_L \quad (11)$$

The function  $C_{\max}$  is the maximum mean-line ordinate for  $C_L = 1.0$  in two-dimensional flow. For other chordwise positions, the three-dimensional cambers will be normalized by the maximum camber; i.e.,

$$f(r, x_c) = \frac{f_p(r, x_c)}{f_p(r, x_{\max})} \quad (12)$$

Correction factors for the ideal angle due to loading can be formed in the same way as the camber correction factor.

$$k_\alpha(r) = \frac{\alpha_i(r)}{\alpha_{i,0} C_L} = \frac{1}{\alpha_{i,0} C_L} \times \int_0^1 \left[ \frac{U_n}{V_r}(r, x) - \frac{U(r)}{V_r} \right] dx \quad (13)$$

where  $\alpha_{i,0}$  is the two-dimensional ideal angle of attack for  $C_L = 1.0$  for the NACA  $a = 0.8$  mean line.

#### Thickness

Blade thickness effects are determined by introducing a source-sink system distributed over the lifting surface [21]. The induced velocity field is given by

$$\left( \frac{V_i(P)}{V} \right)_{\text{thickness}} = \int_{r_A}^1 \int_{\theta_l(r)}^{\theta_u(r)} \sigma(r_0, \theta_0) \times H_i(P, r_0, \theta_0) \left| \frac{\partial x_c}{\partial \theta_0} \right| d\theta_0 dr_0 \quad (14)$$

where  $H_i$  is the velocity induced at the point  $P$  by a unit source located at point  $r, \theta$ ; i.e.

$$H_i = \sum_{m=1}^Z \text{grad} \left( \frac{-1}{4\pi S} \right)$$

and where  $dx_c$  is the element of blade chord, and  $\sigma(r, \theta)$  is the source strength. It is assumed that the source strength distribution is known and is that derived by the usual linear approximations from airfoil theory; i.e.

$$\sigma(r_0, \theta_0) = \frac{V_r}{V} \frac{\partial l(r_0, x_c)}{\partial x_c} = \left( \frac{r_0}{\lambda_s} - \frac{U_T}{V} \right) \frac{1}{\cos \beta_i} \frac{\partial l(r_0, x_c)}{\partial x_c} \quad (15)$$

where  $l(r_0, x_c)$  is the thickness distributed along the chord  $x_c$ ,  $U_T$  is the tangential induced velocity, and  $\lambda_s$  is the apparent advance ratio of the propeller; i.e.,  $V/\pi n D$ .

As for the effect of loading, only the axial and tangential induced velocity components are required from equation (14). If the change in camber along the chord  $x_c$  due to thickness is  $f_{p_i}(r, x_c)$ , and the ideal angle induced by thickness is  $\alpha_i(r)$ , the linearized boundary condition on the blade is

$$\alpha_i(r) + \frac{\partial f_{p_i}}{\partial x_c}(r, x_c) = \frac{U_{n_i}}{V_r}(r, x_c) \quad (16)$$

where  $U_{n_i}$  is the induced velocity normal to the section chord from equation (14) and where  $\alpha_i(r) = \tan \alpha_i(r)$ . Equation (16) is similar to equation (1), and the change in curvature due to thickness is found by integrating equation (16) in the manner of equation (9).

To facilitate evaluating the integrals of equation (14), Kerwin and Leopold [21] used a distribution of quadrilateral source elements over the blades. This approach is similar to that of Hess and Smith [24] for potential flow about arbitrary bodies, except that the elements are placed along the chord rather than over the surface. Therefore, the source-sink distribution is not continuous but is made up of discrete elements. If a sufficient number of elements are used to describe the surface, the accuracy should be good.

Calculations have shown that thickness induces an inflow angle and a camber change but that camber alteration is small [21] except for very small pitch ratios. This flow distortion requires an increase in blade angle (ideal angle) to maintain the desired loading. Correction factors for this ideal angle can be made independent of the magnitude of thickness by dividing the angle (in radians) by the blade thickness fraction for which the calculations were made; e.g.

$$k_i(r) = \frac{1}{BTF} \int_0^1 \frac{U_{\infty}}{V_r} (r, x_c) dx_c \quad (17)$$

where *BTF* is the blade thickness fraction. A camber correction due to thickness can be formed in a similar manner, but since the correction is small it will be ignored. It should be noted from equation (17) that  $k_i(r)$  is also a function of the propeller loading since  $V_r$  is a function of the loading. This effect is small, however, and no correction will be made in the results which are presented.

#### Problems in Numerical Evaluation

Because of their complexity, the expressions arising in the lifting surface calculation procedure described in this paper were necessarily evaluated by digital computation. This resulted in repeated numerical operations to obtain discrete values of the functions involved and the occurrence of inaccuracies, which were dependent upon the characteristics of the functions themselves and were not always predictable by the program user.

The Cheng computer program, described in reference [12], offers many input and output data options which are helpful in describing propellers with special geometries and loadings. This flexibility, however, can lead to inaccuracies in the calculations. Points which merit special attention in both the operation of the program and the analysis of the results are:

1 The computer program, as listed in Appendix B of reference [12], must be modified slightly to give correct results. The convergence criteria

cited in Fortran statements 201 to 204 of Subroutine SUB3 should read 0.9999 and 0.0001 respectively, rather than 0.99 and 0.01. This oversight results in considerable differences in calculated camber values when compared to results of the former program [11] for constant chordwise loading cases.

2 Initial input to the Cheng program is the designation of a fan angle and grid spacing which govern the location and number of control points. The fan angle input must contain the projected view of the propeller blade, and the grid spacing in that fan should be as fine as possible for the greatest accuracy in flow calculation at the control points. The total number of chordwise stations on either side of the control point, however, cannot exceed 90. In order to meet these restrictions, the angle and grid spacing should be carefully checked before each propeller calculation, and particular care should be taken for large blade areas and highly skewed propellers. No automatic checks exist in the program to assume this task.

3 Most critical of the input parameters is the specification of chord-wise coordinates at which the camber and induced velocities will be calculated. Considerable differences in calculated induced velocities appear for relatively small abscissa changes along the chord near the leading and trailing edges. The inclusion of these changes in the resulting integrals yield rather small percent changes in camber but relatively large percent changes in ideal angle. The series discussed in this paper was calculated with chordwise coordinates specified from 5.0 to 95.0-percent chord. Questionable ideal angle and camber corrections arose occasionally for small blade areas and/or low pitch ratios. A change of chordwise coordinates to a range from 2.0 to 98.0 percent chord improved upon the erratic results in these regions, but, for consistency in the series data, these calculated values are not presented. It should be noted also that the questionable data were obvious only in comparisons to other data in the series, alone they perhaps would have gone unnoticed. Independent propeller calculations should be checked against the series presented in this paper or other similar designs if possible.

4 Lifting-surface correction data are given herein only at radial positions  $r/R = 0.3$  through  $r/R = 0.9$  for 0.2R hub propellers. The lifting-surface calculations were made also at  $r/R = 0.25$  and  $r/R = 0.95$ . However, the results were questionable which is probably due to a combination of numerical difficulties involving the singularities at the blade hub and tip.

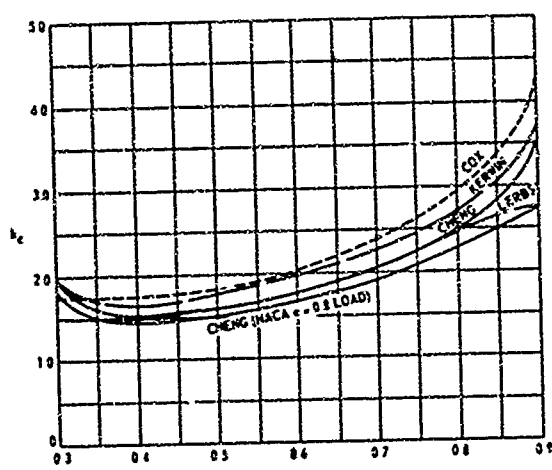


Fig. 3 Comparison of camber correction factors for three blades,  $\pi\lambda_1 = 1.0472$ , and  $A_R/A_0 = 0.75$

### Presentation of the Series

#### Procedure

The propellers for the series were free-running propellers of constant hydrodynamic pitch with a hub diameter of 0.2 of the propeller diameter. Lifting-line calculations were from a computer program based on the induction-factor method of Lerbs [25]. With loading and pitch distributions available from the lifting-line calculations, lifting-surface calculations for loading were made using the program developed by Cheng [12] and for thickness using the program developed by Kerwin and Leopold [21]. These have been combined into one program at NSRDC for running on the IBM-7090 computer.

Because of the complicated nature of the numerical procedures, it is difficult to state the accuracy of the results. To this end, calculations were made and compared in Fig. 3 to those of Cox [5], Kerwin [13], and Lerbs et al. [10] for a three-bladed propeller with an induced advance coefficient<sup>3</sup>  $\lambda_1$  of 0.3333, expanded area ratio of 0.75, and a constant chordwise load distribution. The camber correction factors,  $k_c(r)$ , calculated using results of the Cheng method are within 1 percent of those derived from the Lerbs method for radii between 0.4 and 0.8 but deviate considerably at the 0.3 and 0.9 radii. Both the Cox and the Kerwin methods give correction factors which are, in general, higher than those obtained by the Lerbs and the Cheng methods. These comparisons are consistent with the way Cox and Kerwin arrive at their camber correction factors [10].

<sup>3</sup> The induced advance coefficient  $\lambda_1$  is related to the hydrodynamic pitch ratio by  $\pi\lambda_1 = r \tan\beta_1 = (P/D)_1$ .

Since the calculations are based on similar procedures, the reason for the difference between the results of Lerbs and Cheng is not known. The difference toward the blade tip is probably caused by different numerical techniques, and the difference toward the root is mainly due to the lifting-line calculations; i.e., induction factors versus Goldstein factors.

For a further comparison of lifting-surface calculations, the camber correction factor for a chordwise load distribution corresponding to a NACA  $a = 0.8$  mean line is also plotted in Fig. 3. It is interesting to note that the camber correction factor for this mean line is everywhere smaller than the corresponding factor for the constant load distribution. The three-dimensional camber is higher, however, since  $C_{max}$  is approximately 23 percent larger for the  $a = 0.8$  than for the  $a = 1.0$  mean line.

Lifting-surface corrections were calculated for propellers with four, five, and six blades, with expanded area ratios from 0.35 to 1.15, with hydrodynamic pitch ratios of 0.4 to 2.0, and with a symmetrical outline and skew angles of 7, 14, and 21 deg. The skew angle  $\theta$ , is defined as the angle between two straight lines in the projected plane—one from the shaft centerline through the midchord at the root section and the other

Table 1 Ordinates for NACA 66 (Mod) Thickness Distribution and NACA  $a = 0.8$  Camber Distribution

Station, $x_c$	Thickness Ordinate, $t/l_{max}$	Camber Ordinate, $f/f_{max}$
0	0	0
0.005	0.0665	0.0423
0.0075	0.0812	0.0595
0.0125	0.1044	0.0907
0.025	0.1466	0.1586
0.05	0.2066	0.2712
0.075	0.2525	0.3657
0.1	0.2907	0.4482
0.15	0.3521	0.5869
0.2	0.4000	0.6993
0.25	0.4363	0.7905
0.3	0.4637	0.8635
0.35	0.4832	0.9202
0.4	0.4952	0.9615
0.45	0.5	0.9881
0.5	0.4962	1.0
0.55	0.4846	0.9971
0.6	0.4653	0.9786
0.65	0.4383	0.9434
0.7	0.4035	0.8892
0.75	0.3612	0.8121
0.8	0.3110	0.7027
0.85	0.2532	0.5425
0.9	0.1877	0.3586
0.95	0.1143	0.1713
0.975	0.0748	0.0823
1.0	0.0333	0

Table 2 Distribution of Blade Chord

$r$	$C(r)$
0.2	1.6338
0.3	1.8082
0.4	1.9648
0.5	2.0967
0.6	2.1920
0.7	2.2320
0.8	2.1719
0.9	1.8931
0.95	1.5302
1.0	0

Table 3 Skew Distribution for 14 Deg Skew and  $\pi\lambda_i$  of 1.2

$r$	Skew $R$
0.2	0
0.3	0.0037
0.4	0.0148
0.5	0.0336
0.6	0.0604
0.7	0.0957
0.8	0.1402
0.9	0.1949
1.0	0.2616

Table 4 Calculated Propellers with Symmetrical Blade Outline for Four, Five, and Six Blades

$\pi\lambda_i$	0.4	0.8	1.2	1.6	2.0
$\frac{A_E}{A_0}$	0.35	0.35	0.35	0.35	0.35
	0.55	0.55	0.55	0.55	0.55
	0.75	0.75	0.75	0.75	0.75
	0.95	0.95	0.95	0.95	0.95
	1.15	1.15	1.15	1.15	1.15

from the shaft centerline through the midchord at the blade tip.

#### Choice of Parameters

Geometric properties of the propeller series were chosen to be consistent with present-day practice. All the propellers were designed to have the same chordwise load distribution as that of the NACA  $a = 0.8$  mean line, i.e., a constant chordwise load from the blade leading edge to 0.8 of the chord, and a constant slope to zero at the trailing edge. This mean line was chosen because viscous effects on its lift are small [26], and hence the potential solution closely approximates the true physical flow. The maximum ordinate of this mean line for a  $C_L = 1.0$ ,  $C_{max}$ , is 0.06790, and the two-dimensional ideal angle of attack for  $C_L = 1.0$ ,  $\alpha_{10}$ , is 1.54 deg [26]. The chordwise thickness distribution chosen was the NACA-66 section, TMB modification [27], which has a desirable pressure distribution. Table 1 indicates the

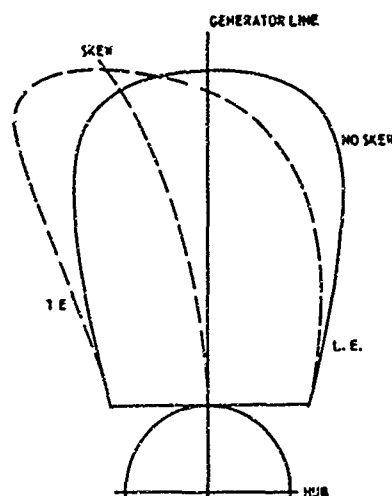


Fig. 4 Expanded blade outlines,  $A_E/A_0 = 0.75$ ,  $Z = 5$ , with symmetrical blade outline and 14-deg skew

half-thickness ordinates as normalized by the maximum thickness. However, the lifting-surface correction for thickness would be expected to be essentially independent of the chordwise thickness distribution, assuming, of course, that the shapes are reasonable.

The spanwise distribution of thickness was assumed to be linear with respect to radius and was given by the following equation:

$$\frac{t_{max}}{D} = (BTF - 0.003)(1 - r) + 0.003 \quad (18)$$

where  $BTF$  is the blade thickness fraction. This choice was based on an examination of a number of propellers of current design.

The blade outlines chosen were slightly wider toward the tip than the Troost outline and were given by

$$c/D = \frac{C(r)}{Z} \left( \frac{A_E}{A_0} \right) \quad (19)$$

where  $C(r)$  is given in Table 2 and  $(A_E/A_0)$  is the expanded area ratio. This is a mathematical outline given by Cox [5] with his constants  $\sigma = 0.732$  and  $\bar{x} = 0.7$ , and is essentially the same outline as given by Schoenherr [28] with his constants  $c = 0.4$  and  $n = 0.3$ . An expanded blade for an  $A_E/A_0$  of 0.75 and five blades is shown in Fig. 4.

The radial distribution of skew was chosen so that the blade-section mid-chord line followed a circular arc in the expanded plane, as shown in Figure 4, and was calculated from the following equation:

Table 5 Correction Factors for Symmetrical Outline,  $Z = 4$

$\lambda_1/\lambda_0$	$\pi\lambda_1 = 0.4$		$\pi\lambda_1 = 0.8$		$\pi\lambda_1 = 1.2$		$\pi\lambda_1 = 1.6$		$\pi\lambda_1 = 2.0$	
	$k_c$	$k_t$	$k_c$	$k_t$	$k_c$	$k_t$	$k_c$	$k_t$	$k_c$	$k_t$
$\lambda_1/\lambda_0 = 0.35$										
$r = 0.3$	1.183	1.180	1.140	1.132	1.176	1.166	1.212	1.203	1.241	1.215
$r = 0.4$	1.016	1.182	1.042	1.172	1.078	1.199	1.114	1.230	1.175	1.117
$r = 0.5$	1.016	1.112	1.035	1.171	1.078	1.204	1.114	1.246	1.118	1.124
$r = 0.6$	1.035	1.142	1.058	1.193	1.117	1.210	1.151	1.261	1.140	1.125
$r = 0.7$	1.097	1.180	1.132	1.215	1.183	1.230	1.187	1.281	1.185	1.127
$r = 0.8$	1.213	1.251	1.256	1.266	1.262	1.304	1.260	1.318	1.262	1.267
$r = 0.9$	1.323	1.340	1.409	1.456	1.513	1.560	1.598	1.653	1.682	1.700
$\lambda_1/\lambda_0 = 0.55$										
$r = 0.3$	1.335	1.713	1.287	1.507	1.370	1.518	1.439	1.466	1.399	1.411
$r = 0.4$	1.035	1.344	1.058	1.378	1.100	1.394	1.232	1.394	1.259	1.353
$r = 0.5$	1.036	1.255	1.059	1.343	1.120	1.376	1.253	1.404	1.257	1.350
$r = 0.6$	1.050	1.201	1.072	1.312	1.135	1.357	1.281	1.424	1.305	1.440
$r = 0.7$	1.103	1.253	1.132	1.442	1.187	1.477	1.378	1.493	1.385	1.514
$r = 0.8$	1.208	1.303	1.247	1.535	1.256	1.569	1.519	1.611	1.515	1.612
$r = 0.9$	1.378	2.033	1.493	1.895	1.594	1.854	1.891	1.894	1.872	1.870
$\lambda_1/\lambda_0 = 0.75$										
$r = 0.3$	1.629	2.218	1.540	1.941	1.640	1.819	1.783	1.724	1.703	1.652
$r = 0.4$	1.116	1.617	1.057	1.711	1.130	1.815	1.643	1.649	1.495	1.656
$r = 0.5$	1.056	1.399	1.029	1.591	1.078	1.676	1.491	1.655	1.454	1.645
$r = 0.6$	1.153	1.316	1.058	1.502	1.124	1.678	1.479	1.712	1.511	1.716
$r = 0.7$	1.318	1.507	1.178	1.684	1.273	1.749	1.605	1.786	1.622	1.815
$r = 0.8$	1.540	1.781	1.399	1.956	1.503	1.886	1.814	1.925	1.615	1.935
$r = 0.9$	2.420	2.532	2.359	2.556	2.360	2.320	2.337	2.527	2.517	2.537
$\lambda_1/\lambda_0 = 0.95$										
$r = 0.3$	2.051	2.745	1.939	2.553	1.953	2.130	2.057	2.015	2.161	1.937
$r = 0.4$	1.255	2.152	1.143	2.076	1.156	2.025	1.642	1.948	1.711	1.916
$r = 0.5$	1.235	1.722	1.121	1.921	1.156	1.846	1.541	1.945	1.691	1.927
$r = 0.6$	1.325	1.615	1.148	1.888	1.157	1.890	1.717	2.016	1.734	2.014
$r = 0.7$	1.444	1.637	1.235	1.980	1.235	2.076	1.875	2.112	1.892	2.135
$r = 0.8$	1.875	2.004	1.735	2.108	1.235	2.237	2.123	2.271	2.140	2.387
$r = 0.9$	2.976	3.023	2.876	2.818	2.431	2.770	2.815	2.805	2.805	2.877
$\lambda_1/\lambda_0 = 1.15$										
$r = 0.3$	2.571	3.314	2.388	2.800	2.376	2.509	2.471	2.433	2.593	2.225
$r = 0.4$	1.774	2.718	1.756	2.635	1.752	2.401	2.471	2.433	2.593	2.225
$r = 0.5$	1.957	2.256	1.756	2.357	1.752	2.401	2.471	2.433	2.593	2.225
$r = 0.6$	2.112	2.112	1.756	2.357	1.752	2.401	2.471	2.433	2.593	2.225
$r = 0.7$	1.837	2.293	1.756	2.357	1.752	2.401	2.471	2.433	2.593	2.225
$r = 0.8$	1.469	3.500	1.756	2.357	1.752	2.401	2.471	2.433	2.593	2.225

Questionable Data

$$\frac{\text{skew}}{R} = R_t - \sqrt{R^2 - (r - 0.2)^2} \quad (20)$$

$$R_t = \frac{0.32}{\text{skew}_{tip}} + \frac{\text{skew}_{tip}}{2}$$

where

$$\text{skew}_{tip} = \frac{\theta_s}{\cos \beta_t}$$

and  $\theta_s$  is the skew angle. As an example, skew in the expanded plane as calculated from this equation is given in Table 3 for a skew angle of 14 deg and a  $\pi\lambda_1 = 1.2$ .

#### Series of Propellers With Symmetrical Blade Outline

The propellers which were calculated for this systematic series are listed in Table 4. Correction factors for camber, ideal angle due to loading,



Table 5 (cont) Correction Factors for Symmetrical Outline,  $Z = 5$

$\lambda_1/\lambda_0 = 0.35$		$\lambda_1/\lambda_0 = 0.4$		$\lambda_1/\lambda_0 = 0.8$		$\lambda_1/\lambda_0 = 1.2$		$\lambda_1/\lambda_0 = 1.6$		$\lambda_1/\lambda_0 = 2.0$	
$r$	$t_c$	$t_c$	$t_c$	$t_c$	$t_c$	$t_c$	$t_c$	$t_c$	$t_c$	$t_c$	$t_c$
0.3	1.136	1.295	1.118	1.240	1.161	1.146	1.171	1.190	1.132	1.177	1.210
0.4	.965	1.086	1.011	1.144	1.030	1.017	1.052	1.101	1.022	1.133	1.202
0.5	.822	1.078	1.035	1.052	1.049	1.017	1.051	1.104	1.019	1.143	1.202
0.6	.707	1.074	1.047	1.062	1.066	1.019	1.054	1.103	1.014	1.170	1.217
0.7	.617	1.071	1.064	1.063	1.063	1.011	1.054	1.103	1.014	1.177	1.217
0.8	.542	1.068	1.064	1.063	1.063	1.011	1.054	1.103	1.014	1.177	1.217
0.9	.483	1.065	1.061	1.060	1.060	1.010	1.053	1.102	1.013	1.176	1.216
$\lambda_1/\lambda_0 = 0.35$		$\lambda_1/\lambda_0 = 0.4$		$\lambda_1/\lambda_0 = 0.8$		$\lambda_1/\lambda_0 = 1.2$		$\lambda_1/\lambda_0 = 1.6$		$\lambda_1/\lambda_0 = 2.0$	
0.3	1.259	1.255	1.253	1.253	1.253	1.253	1.253	1.253	1.253	1.253	1.253
0.4	.965	1.111	1.035	1.144	1.030	1.017	1.052	1.101	1.022	1.133	1.202
0.5	.822	1.078	1.035	1.052	1.049	1.017	1.051	1.104	1.019	1.143	1.202
0.6	.707	1.074	1.047	1.062	1.066	1.019	1.054	1.103	1.014	1.170	1.217
0.7	.617	1.071	1.064	1.063	1.063	1.011	1.054	1.103	1.014	1.177	1.217
0.8	.542	1.068	1.064	1.063	1.063	1.011	1.054	1.103	1.014	1.177	1.217
0.9	.483	1.065	1.061	1.060	1.060	1.010	1.053	1.102	1.013	1.176	1.216
$\lambda_1/\lambda_0 = 0.75$		$\lambda_1/\lambda_0 = 0.95$		$\lambda_1/\lambda_0 = 1.15$		$\lambda_1/\lambda_0 = 1.35$		$\lambda_1/\lambda_0 = 1.55$		$\lambda_1/\lambda_0 = 1.75$	
0.3	1.247	1.247	1.247	1.247	1.247	1.247	1.247	1.247	1.247	1.247	1.247
0.4	.965	1.111	1.035	1.144	1.030	1.017	1.052	1.101	1.022	1.133	1.202
0.5	.822	1.078	1.035	1.052	1.049	1.017	1.051	1.104	1.019	1.143	1.202
0.6	.707	1.074	1.047	1.062	1.066	1.019	1.054	1.103	1.014	1.170	1.217
0.7	.617	1.071	1.064	1.063	1.063	1.011	1.054	1.103	1.014	1.177	1.217
0.8	.542	1.068	1.064	1.063	1.063	1.011	1.054	1.103	1.014	1.177	1.217
0.9	.483	1.065	1.061	1.060	1.060	1.010	1.053	1.102	1.013	1.176	1.216

and ideal angle due to thickness as determined by equations (10), (13), and (17), respectively, are listed in Table 5 for these propellers. These data, in general, are direct computer outputs and are not cross-faired. The data should not be regarded as more accurate than to the second decimal place even though three places are given. Plots of the correction factors versus the propeller

radius are shown in Figs. 5 through 13 for a representative part of the data. Figs. 5, 6, and 7 show the correction factors for a five-bladed propeller with a  $\pi\lambda_1$  of 1.2 for the range of expanded area ratios investigated. Figs. 8, 9, and 10 show the correction factors for a five-bladed propeller with  $\lambda_E/\lambda_0 = 0.75$  for the range of induced advance coefficients investigated. Fi-

Table 5 (cont) Correction Factors for Symmetrical Outline,  $Z = 6$

$A_1/A_0$	$r$	$\alpha_1 = 0.4$		$\alpha_1 = 0.8$		$\alpha_1 = 1.2$		$\alpha_1 = 1.6$		$\alpha_1 = 2.0$	
		$k_c$	$k_t$	$k_c$	$k_t$	$k_c$	$k_t$	$k_c$	$k_t$	$k_c$	$k_t$
$A_1/A_0 = 0.35$	0.3	1.104	.414	1.101	.403	1.123	.440	1.152	.458	1.184	.478
	0.4	.532	.337	1.007	.314	1.112	.323	1.095	.331	1.077	.338
	0.5	1.012	.350	1.066	.336	1.082	.325	1.083	.326	1.076	.327
	0.6	1.012	.350	1.066	.336	1.082	.325	1.083	.326	1.076	.327
	0.7	1.012	.350	1.066	.336	1.082	.325	1.083	.326	1.076	.327
$A_1/A_0 = 0.55$	0.3	1.212	.438	1.235	.413	1.256	.424	1.263	.431	1.277	.430
	0.4	.515	.352	1.025	.329	1.053	.348	1.057	.351	1.056	.350
	0.5	.523	.353	1.047	.323	1.074	.340	1.072	.342	1.071	.341
	0.6	1.016	.372	1.072	.351	1.104	.362	1.102	.361	1.099	.360
	0.7	1.045	.385	1.095	.364	1.124	.373	1.121	.372	1.118	.371
$A_1/A_0 = 0.75$	0.3	1.341	.468	1.364	.443	1.385	.454	1.397	.461	1.409	.458
	0.4	.541	.385	1.057	.362	1.083	.373	1.083	.373	1.083	.373
	0.5	.541	.385	1.057	.362	1.083	.373	1.083	.373	1.083	.373
	0.6	1.045	.405	1.095	.385	1.124	.396	1.121	.395	1.118	.394
	0.7	1.074	.418	1.124	.405	1.153	.416	1.150	.415	1.147	.414
$A_1/A_0 = 0.95$	0.3	1.474	.500	1.497	.475	1.518	.486	1.529	.493	1.540	.490
	0.4	.564	.400	1.076	.385	1.102	.396	1.102	.396	1.102	.396
	0.5	.564	.400	1.076	.385	1.102	.396	1.102	.396	1.102	.396
	0.6	1.074	.420	1.124	.405	1.153	.416	1.150	.415	1.147	.414
	0.7	1.103	.433	1.153	.420	1.182	.431	1.179	.430	1.176	.429
$A_1/A_0 = 1.15$	0.3	1.603	.532	1.626	.507	1.647	.518	1.658	.525	1.669	.532
	0.4	.593	.412	1.106	.397	1.132	.408	1.132	.408	1.132	.408
	0.5	.593	.412	1.106	.397	1.132	.408	1.132	.408	1.132	.408
	0.6	1.106	.432	1.156	.417	1.182	.428	1.179	.427	1.176	.426
	0.7	1.135	.445	1.185	.432	1.212	.443	1.209	.442	1.206	.441

nally, Figs. 11, 12, and 13 show the correction factors for  $\pi\lambda_t = 1.2$  and  $A_R/A_0$  for four, five, and six blades.

In addition to these results, the chordwise distributions of camber, as normalized by the maximum camber, equation (12), are listed in Table 6. Only the normalized coordinates for part of the series are presented since the variation

with the various parameters is small. The data given in this table are direct computer output and, obviously, there are discrepancies at some radii. These radii are marked in the table. The questionable data have been carefully checked and no apparent error could be found. The discrepancies are probably linked to the difficulty encountered in the calculations for low pitch

4

[illegible]

**Spent License Data**

Table 6 (cont) Normalized Chordwise Ordinates,  $f(r, x_c)$ , for Symmetrical Outline,  $Z = 5$ [illegible]

Table 6 (cont) Normalized Chordwise Ordinates,  $f(r, x_c)$ , for Symmetrical Outline,  $Z = 6$ [illegible]

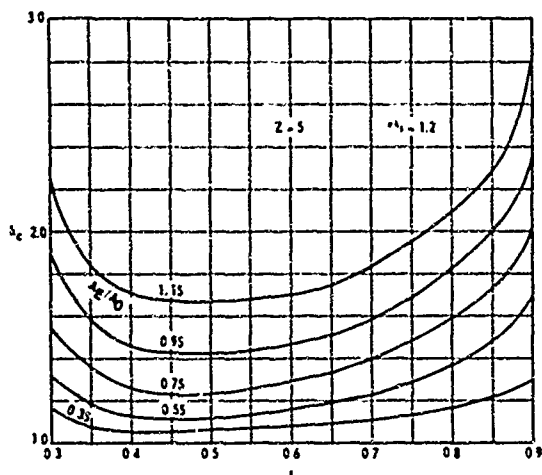


Fig. 5 Camber correction factor for five blades and  $\pi\lambda_1 = 1.2$

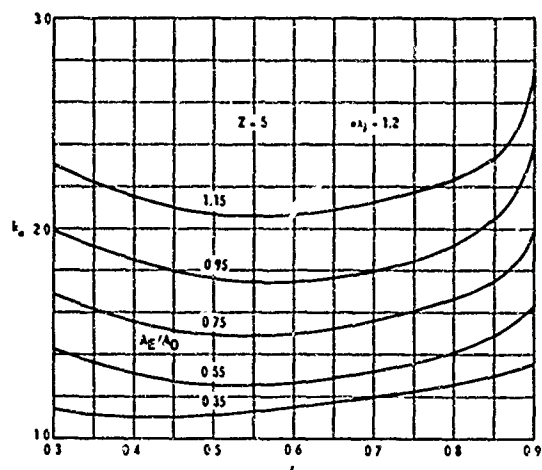


Fig. 6 Correction factor for ideal angle due to loading for five blades and  $\pi\lambda_1 = 1.2$

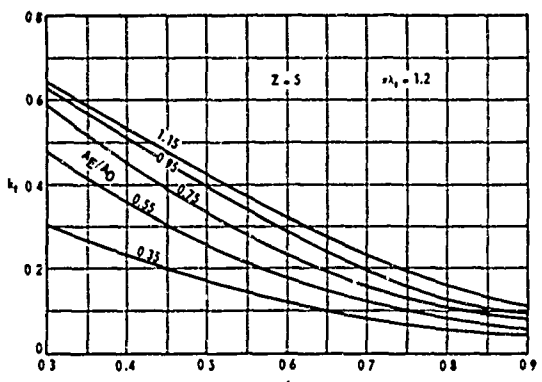


Fig. 7 Correction factor for ideal angle due to thickness for five blades,  $\pi\lambda_1 = 1.2$  and  $BTF = 0.4$

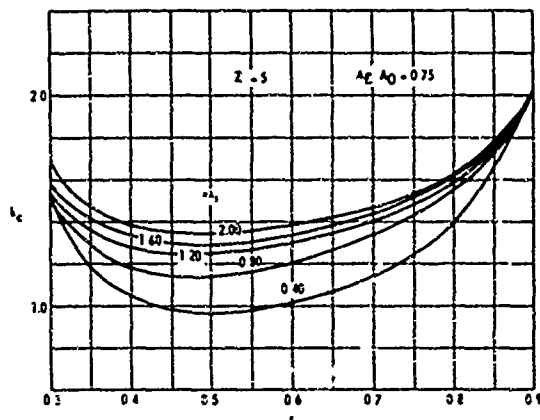


Fig. 8 Camber correction factor,  $k_c(r)$ , for five blades and  $A_E/A_0 = 0.75$

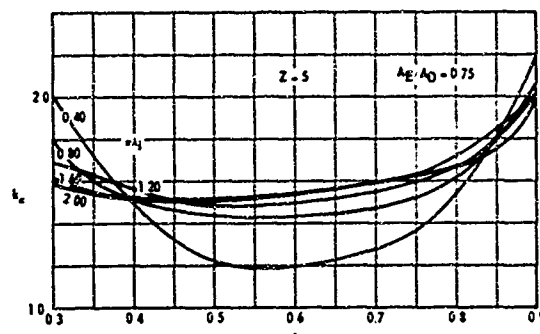


Fig. 9 Correction factor for ideal angle due to loading for five blades and  $A_E/A_0 = 0.75$

ratios and/or small blade areas. Also, all chordwise data should not be regarded as more accurate than to the second decimal place.

A comparison of the chordwise distribution of camber with the two-dimensional value from reference [26] is shown in Table 7 for a typical propeller. The three-dimensional values are flatter near the leading edge and fuller toward the trailing edge of the blade, and the differences decrease slightly toward the blade tip for this propeller. As can be seen from Table 6, there is a tendency for the coordinates to become flatter toward the leading edge with increasing induced advance coefficient and with increasing expanded area ratio. Also, the ordinates become slightly fuller toward the trailing edge for increasing induced advance coefficient, but show little change with area ratio. These data show only slight variation in the spanwise direction, however, and these differences are essentially within the accuracy of the calculations. This leads to the interesting supposition that the normalized camber ordinates are almost independent of their spanwise position.

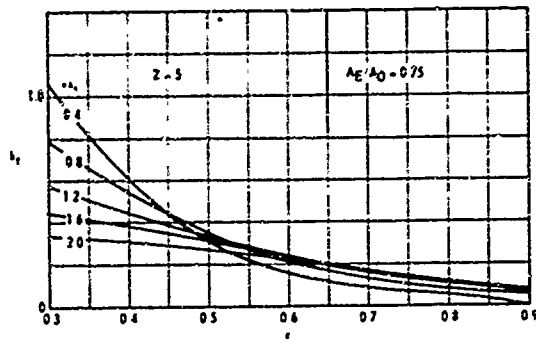


Fig. 10 Correction factor for ideal angle due to thickness for five blades and  $A_E/A_0 = 0.75$

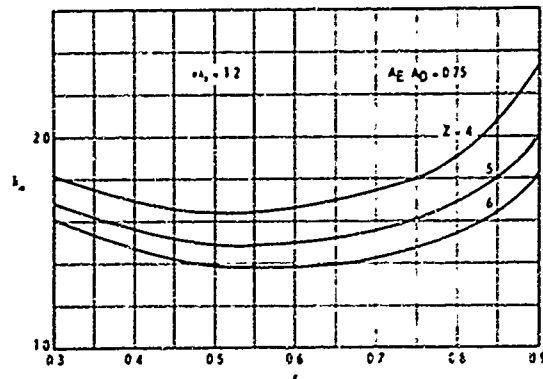


Fig. 12 Correction factor for ideal angle due to loading for  $\pi\lambda_t = 1.2$  and  $A_E/A_0 = 0.75$

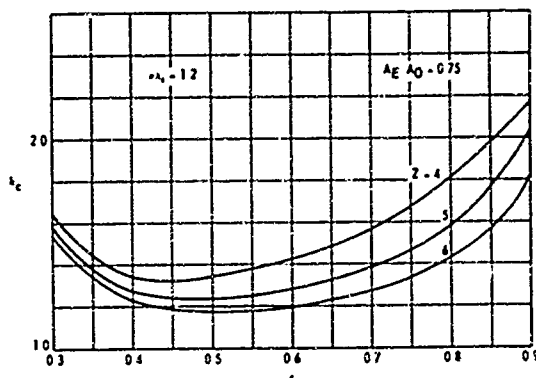


Fig. 11 Camber correction factor for  $\pi\lambda_t = 1.2$  and  $A_E/A_0 = 0.75$

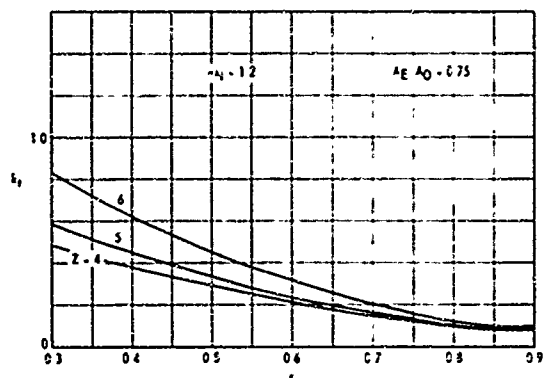


Fig. 13 Correction factor for ideal angle due to thickness for  $\pi\lambda_t = 1.2$  and  $A_E/A_0 = 0.75$

It is quite apparent from Table 5 and Figs. 5, 6, and 7 that the effect of expanded area ratio dominates the correction factors. The correction factors all increase with expanded area ratio for a given number of blades and pitch ratio. In general, the correction factors for camber and

ideal angle due to loading increase with increasing induced advance coefficient, except possibly near the hub and tip of the blades, but decrease for increasing number of blades, i.e., for the range investigated. The factors for camber and ideal

Table 7 Comparison of Chordwise Distributions of Camber for Five Blades,  $\pi\lambda_t = 1.2$ , and  $A_E/A_0 = 0.75$

Chord Position, $x_c$	2-Dimensional Distribution	Distribution for $r = 0.3$	Distribution for $r = 0.6$	Distribution for $r = 0.9$
0	0	0	0	0
0.025	0.159	0.121	0.132	0.133
0.05	0.271	0.230	0.243	0.243
0.1	0.448	0.410	0.424	0.431
0.2	0.699	0.675	0.687	0.698
0.3	0.864	0.856	0.860	0.871
0.4	0.962	0.961	0.963	0.965
0.5	1.000	1.000	1.000	1.000
0.6	0.979	0.977	0.979	0.973
0.7	0.889	0.882	0.889	0.878
0.8	0.703	0.682	0.691	0.682
0.9	0.359	0.364	0.366	0.365
0.95	0.171	0.177	0.177	0.176
0.975	0.082	0.085	0.086	0.082
1.0	0	0	0	0

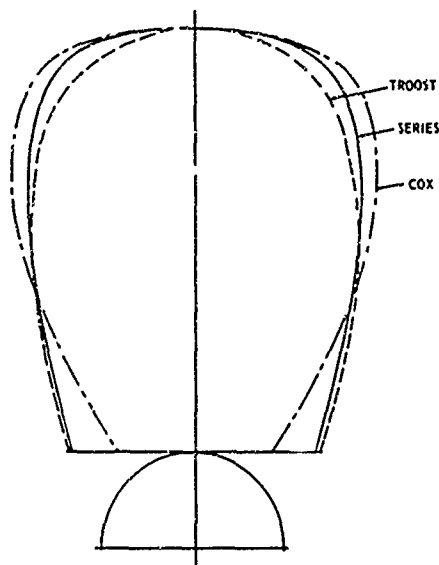


Fig. 14 Comparison of three blade outlines for five-bladed propeller with expanded area ratio of 0.75

angle are greater than unity, except for the higher numbers of blades at low induced advance coefficients. This means that the three-dimensional values are, in general, greater than the two-dimensional values. In most cases, the thickness induces an ideal angle which is largest near the blade root and decreases to negligible values toward the blade tip. In general, this angle decreases with an increasing induced advance coefficient but increases with increasing number of blades.

To show the effect of blade outline, spanwise loading, and spanwise thickness distribution on the correction factors, propellers were calculated in addition to those shown in Table 4. All calculations were for a five-bladed propeller with an induced advance coefficient  $\pi\lambda_i$  of 1.0 and a blade area ratio of 0.75. Two blade outlines, in addition to the one of the series, were investigated; one was the Cox Type 1 and the other was a Troost outline. Fig. 14 compares these outlines, and Figs. 15-17 show the correction factors for the two additional outlines and the series outline. The correction factors generally follow the blade chord distribution, i.e., the blade outline which is narrowest near the root and widest toward the tip (Cox Type 1) has the smallest correction factors near the root and the largest near the tip. Correction factors for the Troost outline, which is the widest near the root and the narrowest toward the tip, show opposite trends. This is true for all three correction factors, except that the ideal angles due to thickness are too small near the

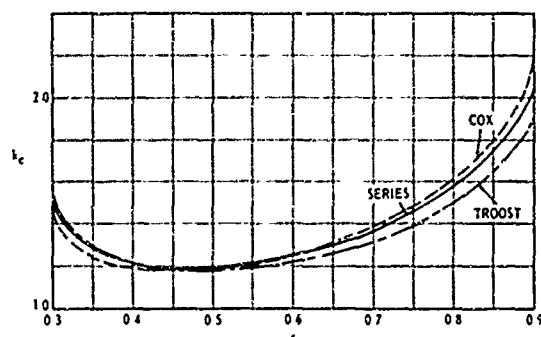


Fig. 15 Comparison of camber correction factors for three blade outlines of Fig. 14

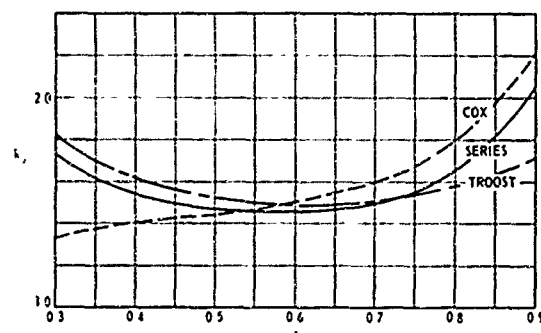


Fig. 16 Comparison of correction factors for ideal angle due to loading for three blade outlines of Fig. 14

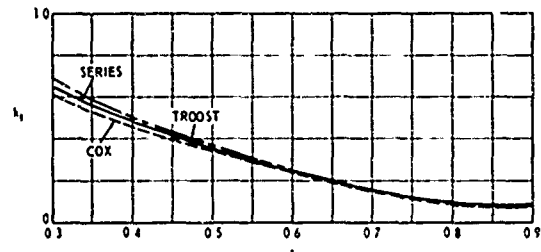


Fig. 17 Comparison of correction factors for ideal angle due to thickness for three blade outlines of Fig. 14

tip to show any such effect. The trends of the correction factors with the blade outlines suggest that correction factors could be approximated from the series for an arbitrary outline by using an "equivalent" area ratio at each radius. The "equivalent" area ratio is defined as the expanded blade area ratio for a propeller of the series which has the same chord at the particular radius in question as the arbitrary outline. Correction factors derived from the series with "equivalent" outlines for the Cox Type 1 and Troost blade shapes were found to be reasonably close to the calculated values, but not in every case were



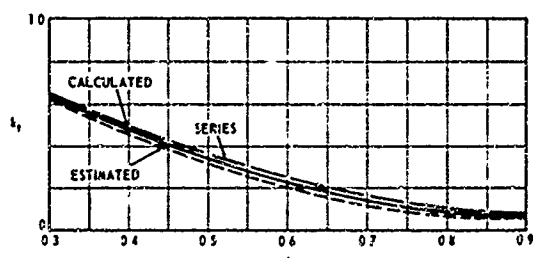


Fig. 18 Comparison of ideal angle correction factors for radial variation in thickness

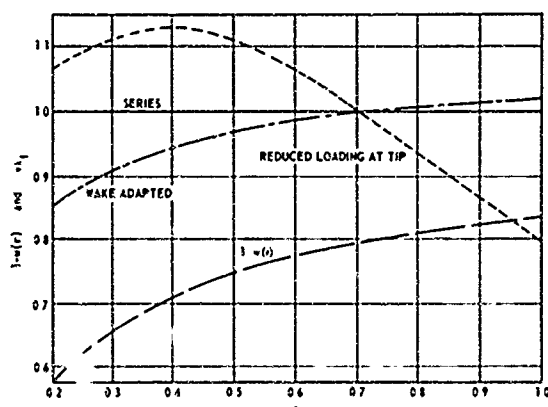


Fig. 19 Comparison of three pitch distributions for five-bladed propeller with expanded area ratio of 0.75

they better than the series data without use of an "equivalent" blade area. Data presented by Cox [5] show similar trends.

Calculations were also made using a nonlinear thickness distribution, and the tabulated thickness values for this variation and the series are shown in Table 8. The relation between the thickness corrections for these two distributions is shown in Fig. 18 for a five-bladed propeller with an induced advance coefficient  $\pi\lambda_t$  of 1.0 and a blade area ratio of 0.75. A curve of the correction factors as estimated from the series data is also shown in this figure. The estimation was made by multiplying the series correction factor by a ratio of the local thickness given in Table 8. As might be expected, the estimation gives a correction which is too low. However, if the correction factors were calculated on the basis of an average of the series and the estimating procedure used, the estimated correction factors would have been extremely close.

The effects of two additional loading variations were also investigated. These loading variations resulted in a distribution of pitch which was not constant. One propeller was a wake-adapted propeller and the other had a reduced loading

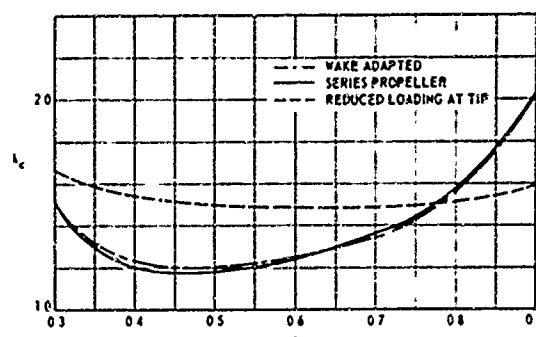


Fig. 20 Comparison of camber correction factors for three pitch distributions of Fig. 19

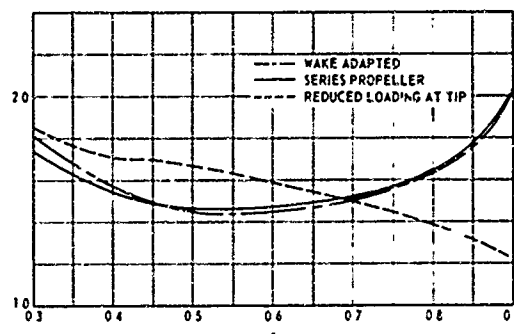


Fig. 21 Comparison of correction factors for ideal angle due to loading for three pitch distributions of Fig. 19

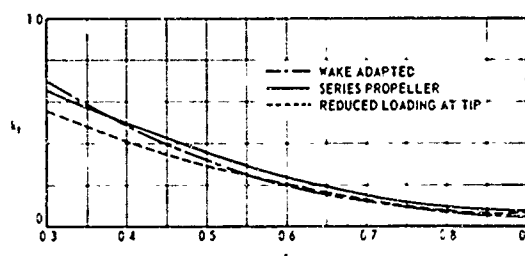


Fig. 22 Comparison of correction factors for ideal angle due to thickness for three pitch distributions of Fig. 19

Table 8 Comparison of Radial Distributions of Thickness

$r$	$(t_{max}/D)$ series	$(t_{max}/D)$
0.2	0.0326	0.03216
0.3	0.0289	0.02761
0.4	0.0252	0.02339
0.5	0.0215	0.01939
0.6	0.0178	0.01572
0.7	0.0141	0.01229
0.8	0.0104	0.00899
0.9	0.0067	0.00592
1.0	0.0030	0.00300

Table 9 Calculated Propellers with Skew

$\frac{\pi\lambda_t}{A_E/A_0}$	0.4			0.8			1.2			2.0		
	0.35	0.75	1.15	0.35	0.75	1.15	0.35	0.75	1.15	0.35	0.75	1.15
$\theta_i$ , deg	7 14 21	7 14 21	7 14 21	7 14 21	7 14 21	7 14 21	7 14 21	7 14 21	7 14 21	7 14 21	7 14 21	7 14 21

at the tip. The resulting pitch distributions are shown in Fig. 19 along with the wake distribution for the wake-adapted propeller. The relation between the correction factors for these two load distributions, as compared to the series results, is shown in Figs. 20, 21, and 22. It is quite apparent that the radial load distribution has a significant effect on the camber and ideal angle due to loading correction factors. These correction factors for the propeller with the reduced loading at the tip are largest toward the blade root and smallest toward the blade tip. The correction factors for the wake-adapted propeller are close to the series results, probably because the radial load distribution is much the same. An attempt was made to estimate the correction factors from Figs. 8, 9, and 10 by entering the figures at the  $\lambda_t$  of each radius for the wake-adapted propeller and that with reduced loading at the tip. Although the values of the correction factors estimated in this manner were, in general, closer to the calculated values, there was not a significant improvement over using the series correction factors directly. The result of the analysis shows clearly that the effect of the radial load distribution is important.

#### Series of Propellers With Skew

The propellers which were calculated with skew are listed in Table 9. Correction factors for camber, ideal angle due to loading, and ideal angle due to thickness, as determined by equations (10), (13), and (17), respectively, are listed in Table 10 for these propellers. As stated for the symmetrical blade outline, the data are not cross-faired and should not be regarded as more accurate than to the second decimal place.

Tables 5 and 10 show that the camber correction factor  $k_c$  is almost independent of skew but that it does tend to increase slightly toward the blade tip above the value for the symmetrical outline for increasing skew. This effect increases slightly with increasing blade area and with increasing induced advance coefficient. The ideal angle correction due to thickness tends to be slightly smaller than the symmetrical outline value. Otherwise, the relationship between this correction factor and skew shows no distinct trend.

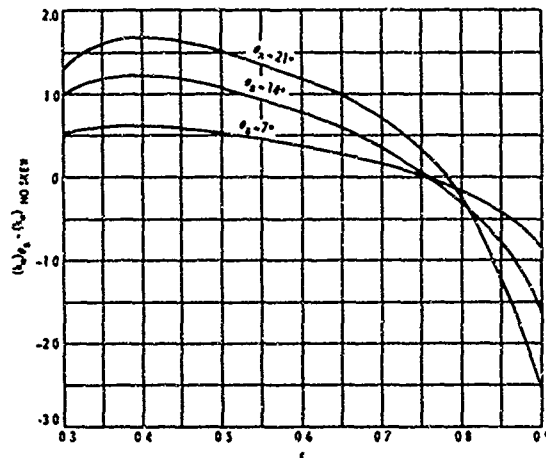


Fig. 23 Ideal angle correction factor induced by skew,  $Z = 5$ ,  $\pi\lambda_t = 1.2$ , and  $A_E/A_0 = 0.75$

The dominant effect of skew is on the ideal angle correction due to loading  $k_a$ . Fig. 23 shows the ideal angle correction factor induced by skew for this series versus the propeller radius for  $Z = 5$ ,  $\pi\lambda_t = 1.2$ , and  $A_E/A_0 = 0.75$ . To obtain this factor, the ideal angle correction factor for the symmetrical outline was subtracted from the correction factor for the skewed outlines. This figure shows that skew effect is significant and induces a positive angle toward the blade root and a negative angle toward the blade tip. This effect has been found by many others [10].

The chordwise distributions of camber, as normalized by the maximum camber, equation (12), are listed in Table 11. Only data for part of the series are presented, as the results are very close to the results obtained for the symmetrical outline. The trends shown by the data for the skewed outline are the same as for the symmetrical outline.

#### Experimental Checks on the Theory

Using lifting-surface theory, several propellers have been designed and tested at NSRDC. None of these has been taken specifically from the series, but the computer programs used in making the lifting-surface calculations were the same as used for the series or were older versions

Table 10 Correction Factors for Skewed Propellers,  $Z = 4$

		$\alpha_1 = 0.4$			$\alpha_1 = 0.8$			$\alpha_1 = 1.2$			$\alpha_1 = 2.0$		
		$k_c$	$k_s$	$k_t$	$k_c$	$k_s$	$k_t$	$k_c$	$k_s$	$k_t$	$k_c$	$k_s$	$k_t$
$\theta_s = 7^\circ, A_E/A_0 = 0.35$													
$r = 0.3$		1.175	1.721	.175				1.175	1.764	.156	1.241	1.793	.126
$r = 0.4$		1.210	1.574	.11				1.059	1.726	.131	1.115	1.797	.131
$r = 0.5$		1.21	1.444	.079				1.075	1.640	.123	1.125	1.739	.120
$r = 0.6$		1.050	1.910	.051				1.119	1.925	.098	1.14	1.634	.102
$r = 0.7$		1.057	1.541	.033				1.175	1.559	.052	1.194	1.490	.051
$r = 0.8$		1.110	1.510	.02				1.272	1.131	.047	1.071	1.114	.052
$r = 0.9$		1.050	1.547	.01				1.517	.570	.040	1.091	.537	.052
$A_E/A_0 = 0.75$													
$r = 0.3$		1.623	2.542	.75	1.345	2.453	.435	1.634	2.357	.355	1.793	2.342	.217
$r = 0.4$		1.11	2.022	.420	1.330	2.308	.354	1.325	2.352	.291	1.451	2.424	.205
$r = 0.5$		1.055	1.747	.275	1.051	2.075	.265	1.349	2.179	.223	1.434	2.315	.150
$r = 0.6$		1.153	1.990	.119	1.335	1.937	.105	1.426	2.059	.154	1.511	2.022	.149
$r = 0.7$		1.05	1.525	.071	1.497	1.795	.102	1.576	1.629	.117	1.627	2.032	.117
$r = 0.8$		1.040	1.05	.045	1.778	1.025	.064	1.10	1.525	.070	1.029	1.525	.065
$r = 0.9$		0.5	1.051	.014	2.404	1.457	.042	2.539	1.351	.057	2.345	1.126	.072
$A_E/A_0 = 1.15$													
$r = 0.3$		1.71	3.7	.31				2.32	3.041	.41	2.537	3.281	.236
$r = 0.4$		1.71	3.7	.27				1.71	3.072	.37	1.976	3.331	.224
$r = 0.5$		1.71	3.7	.21				1.057	3.045	.291	1.945	2.954	.200
$r = 0.6$		1.71	3.7	.1				1.057	2.722	.224	3.019	2.531	.173
$r = 0.7$		1.05	3.113	.17				2.134	2.574	.164	2.197	2.570	.135
$r = 0.8$		1.05	3.10	.10				2.051	2.535	.115	2.901	2.562	.108
$r = 0.9$		0.5	2.705	.064				3.345	2.252	.054	3.307	2.079	.055
$\theta_s = 14^\circ, A_E/A_0 = 0.35$													
$r = 0.3$		1.105	2.031	.154	1.155	2.150	.172	1.175	2.194	.175	1.241	2.274	.115
$r = 0.4$		1.115	1.933	.102	1.042	2.062	.145	1.063	2.000	.134	1.120	2.352	.125
$r = 0.5$		1.230	1.775	.075	1.055	1.930	.116	1.035	2.055	.125	1.131	2.246	.119
$r = 0.6$		1.047	1.691	.050	1.101	1.774	.083	1.102	1.665	.095	1.153	2.059	.099
$r = 0.7$		1.114	1.532	.032	1.177	1.530	.054	1.204	1.545	.055	1.225	1.690	.074
$r = 0.8$		1.032	1.343	.015	1.285	1.103	.034	1.300	1.246	.047	1.325	1.015	.054
$r = 0.9$		1.053	.534	.009	1.337	.183	.024	1.553	.125	.036	1.551	.385	.047
$A_E/A_0 = 0.75$													
$r = 0.3$		1.515	2.292	.720	1.540	2.900	.543	1.532	2.275	.355	1.782	2.904	.235
$r = 0.4$		1.115	2.732	.451	1.235	2.551	.352	1.325	2.942	.291	1.455	3.122	.197
$r = 0.5$		1.055	2.77	.274	1.259	2.545	.255	1.349	2.701	.25	1.452	2.949	.174
$r = 0.6$		1.153	2.350	.117	1.357	2.302	.172	1.451	2.425	.152	1.525	2.709	.144
$r = 0.7$		1.05	1.722	.072	1.539	1.981	.105	1.575	2.020	.115	1.644	2.263	.112
$r = 0.8$		1.05	1.577	.044	1.791	1.495	.057	1.73	1.745	.075	1.254	1.477	.085
$r = 0.9$		0.5	1.170	.011	1.419	.64	.050	2.39	.573	.057	2.365	.328	.052
$A_E/A_0 = 1.15$													
$r = 0.3$		1.71	3.7	.31	2.057	3.554	.571	2.321	3.424	.405	2.522	3.415	.234
$r = 0.4$		1.71	3.927	.27	1.742	3.725	.463	1.725	3.687	.343	1.976	3.780	.224
$r = 0.5$		1.057	3.025	.249	1.746	3.054	.354	1.057	3.576	.279	1.952	3.596	.199
$r = 0.6$		1.05	2.630	.11	1.05	3.002	.252	1.055	3.130	.215	2.025	3.558	.167
$r = 0.7$		1.05	2.657	.17	2.016	2.656	.157	2.134	2.789	.159	2.211	2.937	.132
$r = 0.8$		1.05	2.627	.079	2.01	2.102	.105	2.053	2.195	.113	2.523	2.166	.103
$r = 0.9$		0.5	1.914	.052	3.221	1.413	.075	3.359	1.216	.079	3.342	.775	.054
$\theta_s = 21^\circ, A_E/A_0 = 0.35$													
$r = 0.3$		1.105	2.244	.15				1.175	2.497	.156	1.241	2.501	.103
$r = 0.4$		1.115	2.243	.110				1.059	2.581	.151	1.120	2.755	.117
$r = 0.5$		1.05	2.056	.077				1.099	2.405	.132	1.149	2.653	.111
$r = 0.6$		1.05	1.970	.051				1.151	2.189	.097	1.156	2.425	.094
$r = 0.7$		1.100	1.700	.031				1.237	1.789	.066	1.272	1.967	.071
$r = 0.8$		1.050	1.574	.017				1.335	1.054	.045	1.334	1.110	.050
$r = 0.9$		1.054	.152	.009				1.550	.514	.027	1.601	.1098	.038
$A_E/A_0 = 0.75$													
$r = 0.3$		1.515	3.219	.730	1.540	3.197	.457	1.628	3.207	.350	1.788	3.255	.195
$r = 0.4$		1.11	3.152	.470	1.237	3.325	.348	1.330	3.435	.257	1.473	3.552	.197
$r = 0.5$		1.051	2.676	.234	1.259	2.959	.233	1.360	3.195	.224	1.474	3.470	.178
$r = 0.6$		1.155	2.394	.126	1.347	2.679	.150	1.442	2.655	.154	1.543	3.157	.146
$r = 0.7$		1.05	2.120	.070	1.519	2.247	.120	1.602	2.365	.113	1.678	2.625	.110
$r = 0.8$		1.050	1.557	.045	1.816	1.480	.052	1.862	1.460	.075	1.902	1.532	.051
$r = 0.9$		2.023	.515	.013	2.477	.150	.040	2.457	.510	.055	2.467	.946	.067
$A_E/A_0 = 1.15$													
$r = 0.3$		2.571	4.264	.915				2.351	3.761	.399	2.521	3.733	.234
$r = 0.4$		1.77	4.457	.710				1.025	4.195	.345	1.994	4.338	.220
$r = 0.5$		1.057	3.704	.511				1.037	3.840	.281	1.958	4.141	.195
$r = 0.6$		1.055	3.179	.337				1.938	3.542	.217	2.038	3.870	.165
$r = 0.7$		1.05	2.549	.180				2.154	3.055	.157	2.231	3.314	.133
$r = 0.8$		2.147	2.082	.084				2.515	2.153	.107	2.553	2.199	.102
$r = 0.9$		2.050	1.098	.062				3.441	.114	.079	3.430	.314	.078

Questionable Data

Table 10 (cont) Correction Factors for Skewed Propellers,  $Z = 5$

		$\alpha_1 = 0.4$			$\alpha_1 = 0.8$			$\alpha_1 = 1.2$			$\alpha_1 = 2.0$		
		$k_c$	$k_u$	$k_t$	$k_c$	$k_u$	$k_t$	$k_c$	$k_u$	$k_t$	$k_c$	$k_u$	$k_t$
$\theta_s = 7^\circ, A_t/A_0 = 0.35$													
$r$	0.3	1.155	1.624	.224				1.139	1.598	.270	1.193	1.657	.215
	0.4	.925	1.467	.162				1.049	1.592	.217	1.092	1.721	.159
	0.5	.992	1.288	.179				1.091	1.512	.169	1.054	1.655	.163
	0.6	1.017	1.295	.052				1.071	1.451	.122	1.111	1.581	.129
	0.7	1.042	1.254	.03				1.113	1.340	.068	1.172	1.521	.059
	0.8	1.115	1.172	.025				1.232	.963	.059	1.723	1.647	.071
	0.9	1.333	.974	.023				1.367	.555	.041	1.362	.591	.052
$A_t/A_0 = 0.75$													
$r$	0.3	1.047	2.377	1.535	1.495	2.276	.744	1.559	2.219	.562	1.677	2.235	.590
	0.4	1.097	2.016	.375	1.169	2.143	.922	1.292	2.176	.455	1.375	2.256	.511
	0.5	.954	1.655	.25	1.143	1.915	.349	1.237	2.025	.323	1.346	2.195	.260
	0.6	1.075	1.508	.158	1.175	1.753	.225	1.265	1.894	.225	1.374	2.095	.204
	0.7	1.154	1.432	.072	1.307	1.619	.131	1.392	1.754	.154	1.472	1.967	.159
	0.8	1.372	1.437	.056	1.534	1.457	.079	1.507	1.474	.102	1.620	1.805	.112
	0.9	2.099	1.375	.035	2.052	1.354	.055	2.046	1.162	.075	2.041	.999	.091
$A_t/A_0 = 1.15$													
$r$	0.3	1.042	3.344	1.27				2.226	2.799	.651	2.355	.65	.357
	0.4	1.574	2.337	.255				1.737	2.720	.547	1.742	2.736	.357
	0.5	1.356	2.479	.657				1.850	3.011	.437	1.761	2.717	.265
	0.6	1.333	2.145	.47				1.895	2.468	.324	1.511	2.613	.203
	0.7	1.304	1.821	.209				1.825	2.350	.229	1.932	2.430	.159
	0.8	1.617	1.727	.093				2.109	2.027	.155	2.163	2.030	.140
	0.9	2.032	2.196	.081				2.132	1.830	.115	2.753	1.670	.111
$\theta_s = 14^\circ, A_t/A_0 = 0.35$													
$r$	0.3	1.136	1.662	.293	1.112	1.955	.305	1.161	1.781	.278	1.193	2.111	.203
	0.4	.985	1.810	.179	1.011	1.975	.217	1.032	2.039	.215	1.069	2.253	.135
	0.5	.992	1.633	.106	1.045	1.774	.150	1.060	1.934	.161	1.096	2.143	.139
	0.6	1.031	1.591	.083	1.054	1.679	.105	1.086	1.792	.115	1.133	1.997	.123
	0.7	1.055	1.481	.040	1.107	1.559	.065	1.146	1.527	.079	1.256	1.840	.089
	0.8	1.195	1.221	.034	1.205	1.105	.041	1.264	.924	.052	1.355	1.629	.063
	0.9	1.031	.984	.003	1.412	.240	.025	1.408	.045	.035	1.423	.182	.032
$A_t/A_0 = 0.75$													
$r$	0.3	1.347	2.587	1.165	1.493	2.684	.778	1.559	2.659	.555	1.677	2.751	.540
	0.4	1.007	2.537	.630	1.185	2.685	.533	1.292	2.705	.425	1.363	2.923	.210
	0.5	.954	2.091	.333	1.144	2.383	.349	1.242	2.549	.322	1.393	2.814	.259
	0.6	1.029	1.855	.159	1.194	2.134	.220	1.256	2.307	.225	1.398	2.373	.203
	0.7	1.154	1.541	.091	1.517	1.825	.134	1.409	1.955	.147	1.491	2.151	.151
	0.8	1.415	1.454	.054	1.598	1.379	.052	1.507	1.372	.085	1.658	1.365	.109
	0.9	2.099	1.015	.012	2.059	.556	.035	2.075	.312	.077	2.091	.537	.060
$A_t/A_0 = 1.15$													
$r$	0.3	1.042	3.555	1.272	1.175	3.355	.74	2.217	3.315	.604	2.352	3.157	.612
	0.4	1.574	3.579	.293	1.034	3.497	.571	1.707	3.471	.512	1.649	3.557	.369
	0.5	1.354	.860	.713	1.021	3.072	.515	1.636	3.147	.410	1.727	3.272	.315
	0.6	1.273	2.537	.461	1.054	2.745	.341	1.635	2.793	.356	1.116	3.154	.259
	0.7	1.356	2.337	.255	1.595	2.377	.130	1.34	2.922	.216	1.944	2.722	.197
	0.8	1.617	1.627	.115	2.005	1.647	.135	2.123	1.922	.148	2.175	1.957	.147
	0.9	2.099	1.447	.092	2.099	1.036	.11	2.057	.793	.103	2.055	.560	.112
$\theta_s = 21^\circ, A_t/A_0 = 0.35$													
$r$	0.3	1.125	2.203	.275				1.131	2.247	.270	1.192	2.390	.231
	0.4	.925	2.109	.175				1.05	2.357	.228	1.097	2.623	.193
	0.5	1.017	.95	.022				1.071	2.271	.171	1.113	2.540	.156
	0.6	1.029	1.731	.051				1.106	2.113	.120	1.161	2.315	.120
	0.7	1.075	1.705	.03				1.171	1.787	.078	1.255	1.953	.083
	0.8	1.125	1.423	.023				1.320	.999	.048	1.342	1.153	.059
	0.9	1.455	.245	.006				1.494	.473	.034	1.590	.769	.035
$A_t/A_0 = 0.75$													
$r$	0.3	1.347	2.777	1.079	1.490	2.991	.725	1.559	2.867	.522	1.677	3.027	.545
	0.4	1.337	3.056	.517	1.169	3.152	.914	1.262	3.262	.435	1.391	3.462	.311
	0.5	.954	2.484	.326	1.132	2.800	.347	1.257	3.001	.322	1.377	3.307	.260
	0.6	1.027	2.215	.187	1.205	2.517	.219	1.312	2.722	.224	1.424	3.062	.202
	0.7	1.114	1.930	.099	1.33	2.104	.130	1.432	2.27	.147	1.530	2.841	.147
	0.8	1.410	1.825	.054	1.551	1.431	.079	1.625	1.414	.094	1.714	1.479	.104
	0.9	2.130	.472	.018	2.143	.2665	.062	2.154	.446	.070	2.126	.937	.052
$A_t/A_0 = 1.15$													
$r$	0.3	2.442	3.921	1.572				2.218	3.455	.627	2.344	3.464	.380
	0.4	1.574	4.230	1.073				1.714	3.922	.529	1.860	4.109	.357
	0.5	1.364	3.457	.754				1.668	3.621	.420	1.798	3.912	.312
	0.6	1.233	2.927	.477				1.711	3.315	.312	1.739	3.659	.252
	0.7	1.359	2.345	.247				1.652	2.630	.216	1.973	3.133	.190
	0.8	1.617	1.727	.105				2.143	1.954	.144	2.322	2.040	.133
	0.9	2.995	.807	.087				2.905	.016	.109	2.950	.401	.107

Table 10 (cont) Correction Factors for Skewed Propellers,  $Z = 6$

		$\phi_1 = 0.4$			$\phi_1 = 0.6$			$\phi_1 = 1.2$			$\phi_1 = 2.0$		
		$k_c$	$k_s$	$k_t$	$k_c$	$k_s$	$k_t$	$k_c$	$k_s$	$k_t$	$k_c$	$k_s$	$k_t$
$\phi_s = 7^\circ, A_E/A_0 = 0.35$													
$r = 0.3$		1.158	1.421	.355				1.125	1.351	.435	1.163	1.355	.423
$r = 0.4$		.953	1.415	.229				1.023	1.375	.317	1.087	1.358	.243
$r = 0.5$		.379	1.355	.123				1.023	1.498	.225	1.081	1.348	.196
$r = 0.6$		.353	1.222	.075				1.047	1.409	.192	1.092	1.455	.149
$r = 0.7$		1.024	1.231	.344				1.107	1.200	.101	1.111	1.348	.108
$r = 0.8$		1.291	1.343	.027				1.124	1.039	.067	1.189	1.093	.078
$r = 0.9$		1.277	.563	.007				1.256	.656	.049	1.423	.686	.065
$A_E/A_0 = 0.75$													
$r = 0.3$		1.474	2.165	1.400	1.453	2.148	1.040	1.527	2.108	.764	1.630	2.057	.555
$r = 0.4$		.944	1.377	.773	1.122	2.038	.725	1.218	2.104	.597	1.339	2.183	.463
$r = 0.5$		.528	1.345	.396	1.075	1.795	.242	1.175	1.933	.434	1.295	2.037	.367
$r = 0.6$		.335	1.401	.159	1.050	1.647	.296	1.195	1.723	.297	1.332	1.974	.377
$r = 0.7$		1.052	1.337	.113	1.196	1.503	.171	1.353	1.624	.191	1.365	1.775	.199
$r = 0.8$		1.247	1.289	.069	1.375	1.349	.101	1.443	1.373	.122	1.495	1.427	.141
$r = 0.9$		1.354	1.354	.001	1.855	1.137	.051	1.940	1.054	.091	1.830	.850	.111
$A_E/A_0 = 1.15$													
$r = 0.3$		2.331	3.069	1.698				2.157	2.657	.870	2.259	2.946	.827
$r = 0.4$		1.447	2.826	1.280				1.645	2.732	.711	1.777	2.735	.689
$r = 0.5$		1.211	2.303	.689				1.537	2.469	.595	1.584	2.579	.622
$r = 0.6$		1.113	1.943	.350				1.543	2.297	.412	1.581	2.452	.339
$r = 0.7$		1.140	1.379	.289				1.627	2.083	.227	1.759	2.259	.257
$r = 0.8$		1.435	1.476	.128				1.252	1.839	.185	1.938	1.902	.186
$r = 0.9$		2.432	1.904	.093				2.462	1.586	.124	2.475	1.499	.149
$\phi_s = 14^\circ, A_E/A_0 = 0.35$													
$r = 0.3$		1.104	1.717	.372	1.101	1.872	.475	1.126	1.925	.435	1.154	1.927	.302
$r = 0.4$		.952	1.740	.219	1.010	1.856	.311	1.027	1.997	.318	1.094	2.055	.255
$r = 0.5$		.379	1.525	.124	1.038	1.753	.197	1.034	1.833	.225	1.094	2.014	.203
$r = 0.6$		1.022	1.535	.372	1.030	1.631	.123	1.051	1.732	.152	1.113	1.881	.151
$r = 0.7$		1.024	1.440	.345	1.025	1.433	.078	1.133	1.409	.100	1.144	1.632	.105
$r = 0.8$		1.115	1.151	.075	1.168	1.054	.049	1.184	1.069	.064	1.213	1.065	.072
$r = 0.9$		1.314	.531	.004	1.322	.353	.025	1.331	.142	.044	1.498	.564	.052
$A_E/A_0 = 0.75$													
$r = 0.3$		1.474	2.458	1.422	1.453	2.554	1.030	1.527	2.530	.764	1.630	2.537	.499
$r = 0.4$		.944	2.412	.703	1.129	2.528	.714	1.223	2.683	.589	1.347	2.623	.438
$r = 0.5$		.528	1.930	.420	1.064	2.267	.471	1.181	2.492	.431	1.305	2.704	.358
$r = 0.6$		.335	1.747	.212	1.107	2.021	.293	1.205	2.211	.297	1.319	2.507	.272
$r = 0.7$		1.052	1.549	.115	1.220	1.731	.172	1.350	1.659	.192	1.391	2.094	.195
$r = 0.8$		1.247	1.272	.055	1.399	1.504	.101	1.465	1.353	.123	1.530	1.385	.133
$r = 0.9$		1.354	.721	.009	1.881	.455	.072	1.877	.245	.097	1.880	.612	.102
$A_E/A_0 = 1.15$													
$r = 0.3$		2.331	3.371	1.687	2.115	3.172	1.225	2.149	3.050	.870	2.259	3.220	.815
$r = 0.4$		1.447	3.490	1.315	1.555	3.363	.993	1.552	3.355	.737	1.526	3.334	.655
$r = 0.5$		1.211	2.820	.939	1.449	2.911	.745	1.557	3.012	.565	1.471	2.904	.600
$r = 0.6$		1.113	2.332	.587	1.398	2.574	.512	1.550	2.741	.432	1.490	2.637	.426
$r = 0.7$		1.140	1.818	.309	1.531	2.173	.315	1.636	2.350	.295	1.590	2.340	.250
$r = 0.8$		1.435	1.397	.139	1.744	1.669	.162	1.871	1.752	.168	1.791	1.676	.177
$r = 0.9$		2.432	1.260	.116	2.494	.902	.131	2.496	.714	.129	2.534	.399	.132
$\phi_s = 21^\circ, A_E/A_0 = 0.35$													
$r = 0.3$		1.104	1.765	.355				1.125	2.167	.442	1.188	2.157	.315
$r = 0.4$		.962	2.011	.215				1.033	2.332	.324	1.103	2.425	.262
$r = 0.5$		.379	1.735	.123				1.049	2.295	.227	1.112	2.375	.207
$r = 0.6$		1.017	1.787	.071				1.093	2.045	.151	1.141	2.245	.152
$r = 0.7$		1.057	1.550	.344				1.165	1.656	.095	1.198	1.934	.105
$r = 0.8$		1.164	1.331	.227				1.240	1.159	.051	1.291	1.246	.085
$r = 0.9$		1.357	.432	.004				1.423	.281	.044	1.624	.1002	.039
$A_E/A_0 = 0.75$													
$r = 0.3$		1.474	2.632	1.475	1.453	2.779	1.013	1.527	2.801	.763	1.630	2.804	.481
$r = 0.4$		.944	2.571	.721	1.129	2.987	.710	1.232	3.156	.595	1.354	3.318	.432
$r = 0.5$		.513	2.275	.436	1.092	2.687	.462	1.195	2.695	.429	1.319	3.202	.357
$r = 0.6$		.305	2.094	.215	1.117	2.405	.225	1.227	2.630	.294	1.345	2.959	.271
$r = 0.7$		1.052	1.741	.113	1.231	2.045	.167	1.328	2.197	.198	1.436	2.496	.190
$r = 0.8$		1.276	1.487	.071	1.433	1.374	.098	1.513	1.350	.119	1.593	1.541	.128
$r = 0.9$		1.343	.355	.001	1.931	.196	.076	1.943	.443	.093	1.978	.751	.101
$A_E/A_0 = 1.15$													
$r = 0.3$		2.325	3.502	1.698				2.149	3.255	.827	2.251	3.194	.864
$r = 0.4$		1.447	4.077	1.275				1.552	3.875	.702	1.795	3.966	.513
$r = 0.5$		1.211	3.304	.894				1.572	3.491	.559	1.710	3.759	.435
$r = 0.6$		1.113	2.741	.368				1.565	3.165	.414	1.712	3.335	.344
$r = 0.7$		1.140	2.106	.314				1.653	2.697	.264	1.803	3.049	.254
$r = 0.8$		1.435	1.476	.147				1.910	1.814	.183	2.010	1.995	.179
$r = 0.9$		2.493	.617	.082				2.563	.079	.129	2.599	.395	.134

Table 11 Normalized Chordwise Ordinates,  $f(r, x_c)$ , for Skewed Propellers;  $Z = 4$ ,  $A_E/A_0 = 0.75$ 

### Questionable Data

[illegible]

[illegible]



Table 12 Comparison Between Theory and Experiment for a  
Constant Thrust Loading

Propeller	Z	$A_E/A_0$	$P/D$ at $0.7R$	$BTF$	$C_T$	Experi- mental $\lambda_e$ Design $\lambda_e$	Experi- mental $C_p$ Design $C_p$
A	5	1.318	1.473	0.054	0.566	1.013	0.976
B	3	0.606	1.077	0.040	0.563	0.990	1.025
C	3	0.606	1.084	0.080	0.563	0.987	0.989
D	3	0.303	1.086	0.057	0.570	0.995	1.016
F	3	1.212	1.073	0.028	0.549	1.014	0.965
G	5	1.480	1.503	0.036	0.361	1.008	0.971

of the programs. Table 12 compares theoretical and experimental values for six of these propellers, designated A, B, C, D, F, and G; all used the NACA  $a = 0.8$  mean line and had no skew. In general, the theoretical values are within the accuracy of the experiments and within the accuracy with which the blade-section viscous drag can be chosen.

There appears to be a trend for wide-bladed propellers A, F, and G to be slightly over-pitched. Also, the thick propeller C tended to be slightly under-pitched as compared to the propeller of standard thickness, B. It is possible that both of these differences could arise from determination of the section viscous drag from airfoil data. Propellers A, F, and G have blades with thickness-chord ratios lower than those for which experimental data are available, and propeller B has blades with thickness-chord ratios which are higher than common. A further discussion of most of these propellers will be found in reference [29].

### Conclusions

From the numerous calculations made and the series data presented, a number of conclusions can be drawn with reference to lifting-surface corrections for propellers. Many of these conclusions, of course, have been made previously by other investigators.

1 Use of a realistic chordwise load similar to that for an NACA  $a = 0.8$  mean line results in both an induced camber and ideal angle. The camber correction factors for this load distribution are somewhat less than for the constant-load mean line, but, in general, they are greater than unity, i.e., greater than the two-dimensional camber for the same lift. The ideal angle correction factor due to loading is, of course, zero for the constant load.

2 Correction factors can be formed for the camber and ideal angle due to loading which are independent of the magnitude of propeller loading.

3 Thickness induces an angle and a camber,

but the camber correction is negligible except for low pitches.

4 A correction factor can be formed for the ideal angle induced by thickness which is independent of the magnitude of thickness but dependent on the thickness distribution.

5 Correction factors for camber and ideal angle due to loading are largest near the blade tip and smallest at 0.4 and 0.5 radii. They increase with increasing expanded area ratio and, generally, with increasing induced advance coefficient, but they decrease with increasing number of blades.

6 The ideal angle due to thickness is largest near the blade root and decreases to negligible values toward the blade tip. In general, this angle decreases with increasing induced advance coefficient but increases with increasing blade number.

7 The chordwise distribution of camber is somewhat flatter toward the blade leading edge and, in general, fuller toward the trailing edge as compared with the two-dimensional values. The spanwise change in the camber chordwise distribution is small. In practice, the use of the two-dimensional distribution is probably reasonable.

8 The shape of the blade outline has a significant effect on the correction factors for camber and ideal angle due to loading.

9 The spanwise load distribution has a significant effect on the correction factors for camber and ideal angle due to loading.

10 Skew has little effect on the camber and ideal angle due to thickness but has a large effect on the ideal angle due to loading. Skew induces a positive angle near the blade root and a negative angle toward the blade tip.

11 Experimental results indicate that, for a chordwise load distribution corresponding to that of the NACA  $a = 0.8$  mean line, the use of lifting-surface corrections gives propellers which, in general, meet their predicted performance within the accuracy of the experiments and the accuracy

with which the blade-section viscous drag can be chosen.

12 Correction factors derived herein should replace those calculated by less sophisticated methods; for example, those in reference [22].

13 The numerical evaluation of the complicated theoretical equations may lead to solutions which are erroneous, and calculations must be carefully checked.

#### Acknowledgments

The authors appreciate the assistance of many staff members of the Naval Ship Research and Development Center and the Hydrog Aerodynamisk Laboratorium, Lyngby, Denmark. Special mention goes to C. W. Prohaska of Hydrog and to W. E. Cummins and the directorate of NSRDC for their generous support; to J. B. Hadler of NSRDC and H. W. Lerbs of Hamburgischen Schiffbau-Versuchsanstalt for their encouragement; to H. M. Cheng, E. B. Caster, and E. Harley for their valuable assistance on the various computer programs; to G. G. Cox for reviewing the manuscript; and to Mrs. Shirley Childers, Miss Danielle Dubas, and A. A. Campo for preparation of the manuscript. Also, a paper of this type would not have been possible without the services and cooperation of the Northern European University Computing Center, Lyngby, Denmark, and the Applied Mathematics Laboratory of NSRDC in making the lengthy computer calculations.

#### References

- 1 W. J. M. Rankine, "On the Mechanical Principles of the Action of Propellers," *Trans. INA*, vol. 6, 1865, pp. 13-39.
- 2 S. Goldstein, "On the Vortex Theory of Screw Propellers," *Proceedings of The Royal Society*, London, England, Series A, vol. 63, 1929, pp. 440-465.
- 3 H. Ludwig and I. Ginzl, "On the Theory of Screws with Wide Blades" (Zur Theorie der Breitblattschraube), *Aerodynamische Versuchsanstalt*, Gottingen, Germany, Report 44/A/08, 1944.
- 4 J. A. Sorenberg, "Application of Lifting Surface Theory to Ship Screws," *International Shipbuilding Progress*, vol. 7, no. 67, 1960, pp. 99-106.
- 5 G. G. Cox, "Corrections to the Camber of Constant Pitch Propellers," *RINA*, vol. 103, 1961, pp. 227-243.
- 6 P. C. Pien, "The Calculation of Marine Propellers Based on Lifting-Surface Theory," *Journal of Ship Research*, vol. 5, no. 2, 1961, pp. 1-14.
- 7 J. E. Kerwin, "The Solution of Propeller Lifting-Surface Problems by Vortex Lattice Methods," Massachusetts Institute of Technology, Department of Naval Architecture and Marine Engineering, June 1961.
- 8 T. Y. Wu, "Some Recent Developments in Propeller Theory," *Schiffstechnik*, vol. 12, no. 60, 1965, pp. 1-11.
- 9 W. H. Isay, *Propeller Theorie—Hydrodynamische Probleme*, Springer Verlag Publishers, 1964.
- 10 H. W. Lerbs, W. Alef, and K. Albrecht, "Numerical Analyses of Propeller Lifting Surface Theory" (Numerische Auswertungen zur Theorie der Tragenden Fläche von Propellern), *Jahrbuch Schiffbautechnische Gesellschaft*, vol. 58, 1964, pp. 295-318, David Taylor Model Basin Translation 330.
- 11 H. M. Cheng, "Hydrodynamic Aspect of Propeller Design Based on Lifting Surface Theory: Part I—Uniform Chordwise Load Distribution," David Taylor Model Basin Report 1802, 1964.
- 12 H. M. Cheng, "Hydrodynamic Aspect of Propeller Design Based on Lifting Surface Theory: Part II—Arbitrary Chordwise Load Distribution," David Taylor Model Basin Report 1803, 1965.
- 13 J. E. Kerwin and R. Leopold, "A Design Theory for Subcavitating Propellers," *TRANS. SNAME*, vol. 72, 1964, pp. 294-335.
- 14 D. M. Nelson, "A Lifting Surface Propeller Design Method for High Speed Computers," NAVWEPS Report 8442, NOTS TP 3399, 1964.
- 15 D. M. Nelson, "Numerical Results from the NOTS Lifting Surface Propeller Design Method," NAVWEPS Report 8772, NOTS TP 3856, 1965.
- 16 P. Sulmont, "Theoretical Study on Marine Propeller Performance Using the Rheo-Electrical Analogy Technique," Bureau d'Analyse et de Recherche Appliquées, Report on ONR Contract Nonr(G)00018-61, 1961.
- 17 P. Sulmont, "Analog Study of Some Problems Relative to Lifting Surfaces in a Helicoidal Movement," Bureau d'Analyse et de Recherche Appliquées, Report on ONR Contract No. N62558-2997, 1962.
- 18 T. Nishiyama and T. Sasajima, "Induced Curve-Flow Effect in the Lifting Surface Theory of the Widely Bladed Propellers," *Journal of Ship Research*, vol. 11, no. 1, 1967, pp. 61-70.
- 19 L. Malavard and P. Sulmont, "Application of the Lifting Foil Theory Solved by Rheoelectric Analogy to the Calculation and Design of Sub- and Supercavitating Propellers," Bureau d'An-

- alyse et de Recherche Appliquées, Report on ONR Contract N62558-4998, 1967.
- 20 M. T. Murray, "Propeller Design and Analysis by Lifting Surface Theory," *International Shipbuilding Progress*, vol. 14, no. 160, 1967, pp. 433-451.
  - 21 J. E. Kerwin and R. Leopold, "Propeller Incidence Correction due to Blade Thickness," *Journal of Ship Research*, vol. 7, no. 2, 1963, pp. 1-6.
  - 22 M. K. Eckhardt and W. B. Morgan, "A Propeller Design Method," *TRANS. SNAME*, vol. 63, 1955, pp. 325-374.
  - 23 W. B. Morgan and J. W. Wrench, Jr., "Some Computational Aspects of Propeller Design," *Methods in Mathematical Physics*, vol. 4, Academic Press Inc., New York, N. Y., 1965, pp. 301-331.
  - 24 J. L. Hess and A. M. O. Smith, "Calculation of Nonlifting Potential Flow about Arbitrary Three-Dimensional Bodies," Douglas Aircraft Co. Inc. Report E. S. 40622, Long Beach, Calif., 1962.
  - 25 H. W. Lerbs, "Moderately Loaded Propellers with a Finite Number of Blades and an Arbitrary Distribution of Circulation," *TRANS. SNAME*, vol. 60, 1952, pp. 73-117.
  - 26 I. H. Abbott, A. E. von Doenhoff, and L. S. Stivers, Jr., "Summary of Airfoil Data," NACA Report 824, 1945.
  - 27 T. Brockett, "Minimum Pressure Envelopes for Modified NACA-66 Sections with NACA  $a = 0.8$  Camber and BuShips Type I and Type II Sections," David Taylor Model Basin Report 1780, 1966.
  - 28 K. E. Schoenherr, "Propulsion and Propellers," *Principles of Naval Architecture*, vol. 2, edited by H. E. Russell and L. B. Chapman, SNAME, New York, 1939, p. 157.
  - 29 S. B. Denny, "Cavitation and Open Water Performance of a Series of Propellers Designed by Lifting-Surface Methods," NSRDC Report (in preparation).